NATIONAL ADVISORY COMMITTEE FOR AERONAUTICS

TECHNICAL NOTE 3904

INVESTIGATION OF THE EFFECTIVENESS OF

BOUNDARY-LAYER CONTROL BY BLOWING OVER A COMBINATION

OF SLIDING AND PLAIN FLAPS IN DEFLECTING A PROPELLER

SLIPSTREAM DOWNWARD FOR

VERTICAL TAKE-OFF

By Kenneth P. Spreemann and Richard E. Kuhn

Langley Aeronautical Laboratory
Langley Field, Va.

NACA

Washington

December 1956

NATIONAL ADVISORY COMMITTEE FOR AERONAUTICS

TECHNICAL NOTE 3904

INVESTIGATION OF THE EFFECTIVENESS OF

BOUNDARY-LAYER CONTROL BY BLOWING OVER A COMBINATION

OF SLIDING AND PLAIN FLAPS IN DEFLECTING A PROPELLER

SLIPSTREAM DOWNWARD FOR

VERTICAL TAKE-OFF

By Kenneth P. Spreemann and Richard E. Kuhn

SUMMARY

An investigation of the effectiveness of blowing a jet of air over the flaps of a wing equipped with a 50-percent-chord sliding flap and a 25-percent-chord plain flap in deflecting a propeller slipstream downward for vertical take-off has been conducted in a static-thrust facility at the Langley Aeronautical Laboratory. The effects of a leading-edge slat, ground proximity, end plate, and propeller position were also investigated.

The results of the investigation indicated that boundary-layer control is an effective means of maintaining attached flow to flap deflections higher than those which could otherwise be used to provide increases in resultant force and turning angles. Whether it would be more economical to use a part of the available power for boundary-layer control than to apply all of the power to the propellers would appear to depend strongly on the system employed and, for a particular installation, should be determined from a detailed analysis. With flap deflections at which the flow is not separated and at blowing rates above those necessary to maintain attached flow, the only gains in resultant force and turning angle are those due to the direct thrust of the blowing system.

INTRODUCTION

The Langley 7- by 10-Foot Tunnels Branch is conducting an investigation of various wing-flap configurations in an effort to develop relatively simple arrangements capable of deflecting the propeller slipstream downward for vertical take-off. The capabilities of a few of the configurations investigated are reported in references 1 to 4. In these

investigations the tendency of the slipstream to separate from the upper
surface of the wing has limited the turning angles obtained and may be
responsible for some of the losses in resultant force. The investi-
gation discussed herein was undertaken in order to study the effective-
ness of boundary-layer control (blowing air over the flap) as a means of
maintaining attached flow to higher flap deflections than could other-
wise be used. This procedure would increase the downward deflection of
a propeller slipstream.

The sliding-flap configuration of reference 4 was constructed and
a nozzle capable of exhausting a jet of air over the flap was incorpo-
rated. Data for this model without boundary-layer control by blowing
over the flap are presented in reference 4. Much of the data of the
reference paper have been reproduced herein to provide direct comparisons
between data without boundary-layer control and the data from this
investigation with the use of boundary-layer control.

The investigation was conducted in a static-thrust facility at the
Langley Aeronautical Laboratory and employed a model wing equipped with
a 50-percent-chord sliding flap and a 25-percent-chord plain flap.

COEFFICIENTS AND SYMBOLS

The positive sense of forces, moments, and angles used in this
paper are indicated in figure 1. Moments are referred to 0.25 of the
mean aerodynamic chord.

$b/2$ span of semispan wing, 2.0 ft

c_w wing chord, 1.5 ft

c_s slat chord, $0.30c_w$

D propeller diameter, 2.0 ft

h height of wing trailing edge above ground, ft

x longitudinal position of propeller ahead of wing leading
              edge, ft

z vertical position of propeller axis relative to wing chord
              plane, ft (positive downward)

$\delta_{f,1}$ deflection of forward or sliding flap, deg

$\delta_{f,2}$ deflection of rear or plain flap, deg

δ_S slat deflection, deg (positive upward with respect to wing
         chord plane)

L   lift, lb

F_X longitudinal force, lb

M   pitching moment, ft-lb

F   resultant force, lb

T   propeller thrust, 15 lb

θ turning angle, inclination of resultant-force vector from
         thrust axis, $\tan^{-1} L/F_X$, deg

C_μ'' momentum coefficient, $\dfrac{Q_n \rho_n V_n}{q''S}$

C_q'' flow coefficient, $\dfrac{Q_n}{V''S}$

C_p'' pressure coefficient, $\dfrac{P_b - p''}{q''}$

P_b power in blowing system, $\dfrac{\rho_n \frac{t}{12} \frac{b}{2}(V_n)^3}{2}$, ft-lb/sec

P_s power in slipstream, $\dfrac{\rho'' \frac{\pi}{4} D^2 (V'')^3}{4}$, ft-lb/sec

Q_n quantity of air blown out of nozzle, cu ft/sec

ρ_n mass density of air blown out of nozzle, slugs/cu ft

V_n nozzle exit velocity assuming isentropic expansion to slip-
         stream static pressure, ft/sec

ρ'' mass density of air in slipstream, slugs/cu ft

V'' slipstream velocity, ft/sec

q'' slipstream dynamic pressure, $\dfrac{T}{\pi D^2/4}$, lb/sq ft

S wing area of semispan model, 3.0 sq ft

p_b static pressure in blowing system, lb/sq ft

p'' slipstream static pressure, lb/sq ft

t nozzle gap, in.

F_n nozzle thrust, lb

ΔF experimental increment in resultant force with blowing
             system in operation, lb

ΔF_1 increment in resultant force calculated from momentum in
             blowing system, lb

ΔF_2 increment in resultant force obtained by utilizing same
             power required by blowing system in propeller, lb

η'' assumed static-thrust efficiency of propeller

η assumed efficiency of blowing system

$\Delta\theta_\mu$ experimental increment in θ due to blowing system, deg

$\Delta\theta_{\mu,1}$ increment in θ calculated from momentum in blowing system,
             deg

APPARATUS AND METHOD

A drawing of the model with pertinent dimensions is presented in
figure 2, and a photograph of the model mounted for testing is shown in
figure 3. The geometric characteristics of the model are given in the
following table:

Wing:
  Area (semispan), sq ft 3.0
  Span (semispan), ft 2.0
  Chord, ft 1.5
  Airfoil section . . . . NACA 4415

5

Propeller:
  Diameter, ft 2.0
  Nacelle diameter, ft 0.33
  Airfoil section . . . .   Clark Y
  Solidity 0.07

The forward flap, which is referred to as a sliding flap, was
hinged forward of the flap near the lower wing surface at the 35-percent-
chord station (fig. 2(a)). The sliding-ramp radius was 15 percent of
the wing chord and was made tangent to the upper surface of the wing.
The rear flap, a plain flap, was made by sawing off the rear 25 percent
of the wing and reattaching it with a piano hinge at the 75-percent-
chord station. With the flap deflected, the gap at the hinge line was
filled and faired with modeling clay. An end plate made of 1/16-inch
sheet metal was installed at the wing tip (fig. 2(b)).

The leading-edge slat was rolled from 1/16-inch sheet steel to a
contour that corresponded to the upper surface of the wing from the
leading edge to the 30-percent-chord station. For these tests the upper
surface of the wing was not modified, although modification would be
necessary in a practical application in order to retract the slat;
however, it is believed that this difference would have only a small
effect on the results. The slat positions tested are shown in figure 4.
Tests were made with the propeller in two positions; one was at
$x/D = 0.41$, $z/D = 0$ and the other was at $x/D = 0.167$, $z/D = 0.167$.

For these tests, the propeller was mounted independently as shown
in figures 2(a) and 3. The thrust axis was always parallel to the wing
chord plane. The propeller was driven by a variable-frequency electric
motor at about 5,500 rpm, which gave a tip Mach number of approxi-
mately 0.52. The motor was mounted inside an aluminum-alloy nacelle by
means of strain-gage beams in such a way that the propeller thrust and
torque could be measured. The total lift, longitudinal force, and
pitching moment of the model were measured on a strain-gage balance at
the root of the wing.

The ground was simulated by a sheet of plywood as shown in figures 1
and 3. All tests with the ground board were conducted with an angle of
20° between the ground board and thrust axis of the propeller.

The full-span blowing nozzle (approximate chordwise shape shown in
fig. 2(a)) was adjustable by means of jackscrews for gap openings
of 0.006, 0.009, and 0.016 inch. The flow coefficient, pressure coef-
ficient, and ratio of power in the blowing system to power in the slip-
stream plotted against momentum coefficient for the three nozzle gaps
employed in this investigation are presented in figure 5. The mass flow
through the nozzle was measured by means of a standard sharp-edge-orifice
flowmeter. Air was supplied by a 90-pound-per-square-inch 1/2-inch line.

The investigation was conducted in a static-thrust facility at the Langley Aeronautical Laboratory. All data presented were obtained at zero forward velocity with a thrust of 15 pounds from the propeller. Inasmuch as the tests were conducted under static conditions in a large room, none of the corrections that are normally applicable to wind-tunnel tests were employed.

RESULTS AND DISCUSSION

The data are presented in the figures as follows:

Effect of Flap Deflection

From figures 6 to 9 it is seen that without boundary-layer control the resultant-force vector is rotated upward progressively with flap deflections up to 60°. With only the sliding flap deflected and without boundary-layer control, the flap is stalled above a deflection of approximately 50° (fig. 6(c)). With boundary-layer control, achieved by blowing over the flap, the turning angles are greatly increased at the higher flap deflections. It is of significance to note that large increases in turning angles are induced at very low momentum coefficients for the high flap deflections. Evidently these large increases in turning angles are the result of reattaching the slipstream to a stalled flap. For example (see fig. 6(c)), there is little or no gain in turning angles at 20° and 40° flap deflection; however, at 70° and 80°, with only a small quantity of air from the nozzle, the turning angles are increased 15° to 25°.

Similar results are obtained with combined flap deflections when large sliding-flap deflections are employed (figs. 8 and 9); however, if the sliding flap is deflected only 50° (fig. 7) in combination with the

plain flap deflected up to 40°, fairly large turning angles are obtained without boundary-layer control, and large increases in turning angle due to boundary-layer control were not experienced. These facts indicate that the flow over this configuration was not badly separated without boundary-layer control.

Although the turning angles were increased with flap deflections and blowing, the ratio of resultant forces noticeably decreased. These reductions in resultant force with increases in turning angles would be of considerable importance in considering a compromise between flap setting, quantity of blowing, and thrust available for practical use.

Boundary-layer control caused increases in the diving moments for all flap configurations. These increased moments probably resulted from the direct thrust of the boundary-layer air being applied downward in back of the center of gravity and from the reattachment of the flow of air to the flaps which increases the flap effectiveness.

An idea of the power required in the blowing system can be obtained from part (e) of figures 6 to 9. The ratio P_b/P_s represents the ratio of air horsepower in the blowing system to the air horsepower in the slipstream. Most of the gains in turning angle are made at relatively low power ratios. If the blowing air were obtained from an engine-driven compressor system, the brake-horsepower ratios would be higher than the values shown because the efficiency of the blowing system, including duct losses, would probably be less than the static-thrust efficiency of the propeller.

Effects of Proximity to Ground

The effects of height above the ground are shown in figure 10 for various quantities of air blowing over a combination flap deflection of $\delta_{f,1} = 50°$ and $\delta_{f,2} = 40°$. Inasmuch as this flap setting was considered to be one of the better compromise arrangements ($\theta = 58°$ to $70°$, $F/T = 0.84$ to 0.92, fig. 7), it was selected for most of the remainder of the investigation. Large reductions in turning angles and in resultant force were incurred near the ground without boundary-layer control. Application of boundary-layer control, however, only slightly reduced the adverse effects of the ground below a value of h/D of approximately 0.583.

The addition of an end plate (fig. 11) had little effect on the characteristics of the model except that in the position closest to the ground the resultant force was greatly increased. The overall detrimental ground effects were considerably offset by the addition of a leading-edge slat (fig. 12). In figure 13 it is indicated that the leading-edge slat reduced the diving moments to approximately one-half

of those of the basic flap configuration of figure 10, and it is also
indicated in figure 13 that when the slat was being used for control,
the control effectiveness between slat angles (δ_s) of 20° and 30° was
increased by the use of boundary-layer control. References 3 and 4
contain a more comprehensive analysis of the leading-edge slat as a
control device without boundary-layer control.

Effects of Thrust Axis Position and Change in Nozzle Gap

Figures 14 and 15 show the characteristics of the model with the
thrust axis lowered 16.7 percent of the propeller diameter below the
wing chord plane and with the propeller closer to the model leading
edge. By comparing the configurations in figures 14 and 15 with the
configurations in figures 10 and 11, it is noted that when the thrust
axis is lowered and the propeller is closer to the model leading edge,
the diving moments were greatly reduced (from approximately -0.15 and
-0.24 to 0 and -0.05). By comparing figures 12 and 15, it is noted
that the lowering of the thrust axis was more effective than the use of
the leading-edge slat in reducing the diving moments in this investigation.
In figures 11 and 15 it is shown that approximately 15° to 20° increases
in θ are evidenced by lowering the thrust axis without boundary-layer
control. For the configuration in figure 15 the propeller was moved
closer to the model leading edge; however, from previous investigations
(refs. 5 and 6) it was shown that, within the range of x/D and z/D
employed in this investigation, the longitudinal position of the pro-
peller had little effect on M/TD and θ.

Changes in nozzle gap (fig. 16) had negligible effect on the results
for these flap deflections.

ANALYSIS

A brief analysis of the increases in resultant force and turning
angle due to boundary-layer control is presented in figures 17 to 21.
The experimental data, in general, indicate that the action of the
blowing air is primarily to reattach the slipstream to the wing, and
this action thus gives large increases in resultant force and turning
angle at low momentum coefficients; but once the flow is attached, the
only increases in resultant force achieved with increased blowing rates
are due to the direct thrust effects of the blowing air. In order to
check the validity of these ideas, the amount of increase in resultant

force and turning angle due to the direct thrust of the blowing air was calculated (see following sketch):
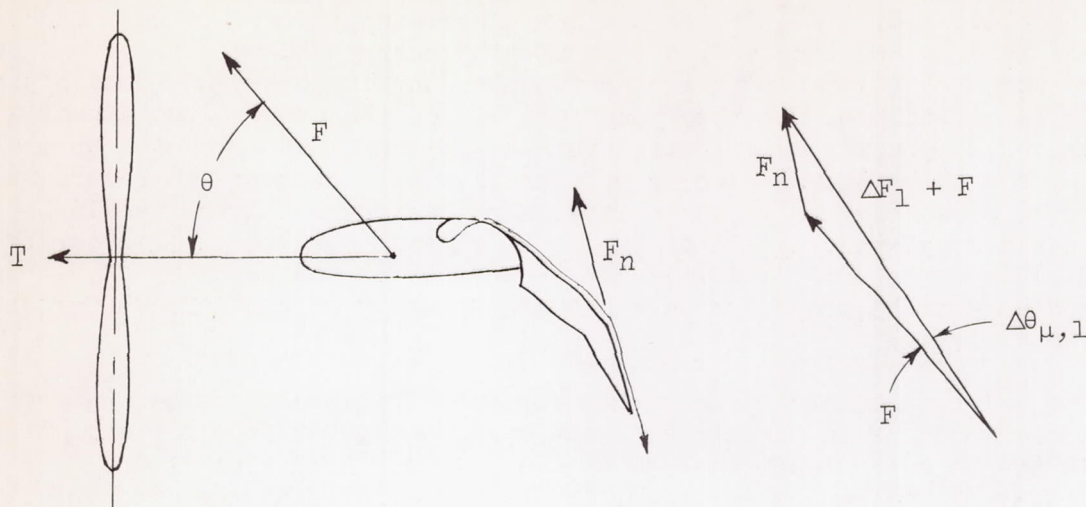
For the calculated increments, all the power from the nozzle is considered to leave the model parallel to the upper surface of the rear flap (the optimum condition that could prevail).

Figure 17 shows the increments in resultant force and turning angle that were obtained from the experimental data compared with those calculated from the power of the blowing system. With a flap deflection of only 20°, the experimental and calculated curves are almost coincident, and this indicates that the flap was not stalled. Consequently, the only gains due to blowing air over the flap are due to the direct thrust of the blowing system. At 70° deflection, however, the experimental data (at low momentum coefficients) exhibit much more rapid increases in both resultant force and in turning angle than the increases predicted by the calculations. The large increases in resultant force and in turning angle are due to the reattachment of the flow to the wing surface. The fact that the experimental and calculated curves are essentially parallel above a momentum coefficient of approximately 0.03 indicates that the only gains incurred above this blowing rate are due to the direct thrust of the blowing system. Similar results are shown for combined flap deflections in figure 18.

In figure 19 the ratio of the increments in resultant force and the increments in turning angle are plotted against flap angle for two momentum coefficients. The effectiveness of the blowing system in reattaching the slipstream to the flap begins to fail between the flap deflections of 70° and 80° even at the higher momentum coefficients.

Figures 17 and 18 show that above the momentum coefficient at which the flow reattaches the only gains received are those due to the direct

jet thrust of the blowing system. Large gains in resultant force in this region therefore require the expenditure of appreciable power in the blowing system. If the boundary-layer-control system were used only for landing and take-off, a form of high-energy low-weight system, such as turbojet engines with a high ratio of thrust to weight, possibly could be employed for this purpose. If, on the other hand, a shaft-driven compressor using power from the main engines were used to provide the boundary-layer-control air, possibly the increments in resultant force thus obtained would be less than the increments that would be obtained by applying all of the power in the propeller. In order to evaluate this idea, the relative efficiency of the boundary-layer-control system and the propeller were assumed to be 50 percent and 75 percent, respectively.

Figures 20 and 21 show that for the efficiencies below C_μ'' of 0.03 there would be an advantage in employing the power from the main engines in the boundary-layer-control system. Above this value it would be more profitable to employ the power in the propeller. Another possibility would be to use the exhaust gases from a turboprop engine in the boundary-layer-control system. The momentum coefficients thus obtained would be low, but it is probable that with proper design the resultant force gained by the boundary-layer-control action would be greater than those gained by the residual thrust of the engine.

CONCLUSIONS

An investigation of the effectiveness of blowing a jet of air over the flaps of a wing equipped with a sliding flap (forward flap) and a trailing plain flap in deflecting a propeller slipstream downward for vertical take-off indicates the following conclusions:

1. Boundary-layer control is an effective means of maintaining attached flow to flap deflections higher than those which could otherwise be used to provide increases in resultant force and turning angles. Whether it would be more economical to use a part of the power for boundary-layer control than to apply all of the power to the propellers would appear to depend strongly on the system employed and, for a particular installation, should be determined from a detailed analysis.

2. With flap deflections at which the flow is not separated and at blowing rates above those necessary to maintain attached flow, the only gains in resultant force and turning angle are those due to the direct jet thrust of the blowing system.

3. Large reductions in turning angles and in resultant force were incurred near the ground; however, the detrimental ground effects were offset by the addition of a leading-edge slat.

4. The leading-edge slat considerably reduced the diving moments; however, lowering the thrust axis 16.7 percent of the propeller diameter below the wing chord plane was more effective.

Langley Aeronautical Laboratory
    National Advisory Committee for Aeronautics,
        Langley Field, Va., October 2, 1956.

<div align="center">REFERENCES</div>

1. Kuhn, Richard E., and Draper, John W.: An Investigation of a Wing-Propeller Configuration Employing Large-Chord Plain Flaps and Large-Diameter Propellers for Low-Speed Flight and Vertical Take-Off. NACA TN 3307, 1954.

2. Kuhn, Richard E., and Draper, John W.: Investigation of Effectiveness of Large-Chord Slotted Flaps in Deflecting Propeller Slipstreams Downward for Vertical Take-Off and Low-Speed Flight. NACA TN 3364, 1955.

3. Kuhn, Richard E.: Investigation at Zero Forward Speed of a Leading-Edge Slat as a Longitudinal Control Device for Vertically Rising Airplanes That Utilize the Redirected-Slipstream Principle. NACA TN 3692, 1956.

4. Kuhn, Richard E., and Spreemann, Kenneth P.: Preliminary Investigation of the Effectiveness of a Sliding Flap in Deflecting a Propeller Slipstream Downward for Vertical Take-Off. NACA TN 3693, 1956.

5. Draper, John W., and Kuhn, Richard E.: Some Effects of Propeller Operation and Location on Ability of a Wing With Plain Flaps to Deflect Propeller Slipstreams Downward for Vertical Take-Off. NACA TN 3360, 1955.

6. Kuhn, Richard E.: Investigation of the Effects of Ground Proximity and Propeller Position on the Effectiveness of a Wing With Large-Chord Slotted Flaps in Redirecting Propeller Slipstreams Downward for Vertical Take-Off. NACA TN 3629, 1956.
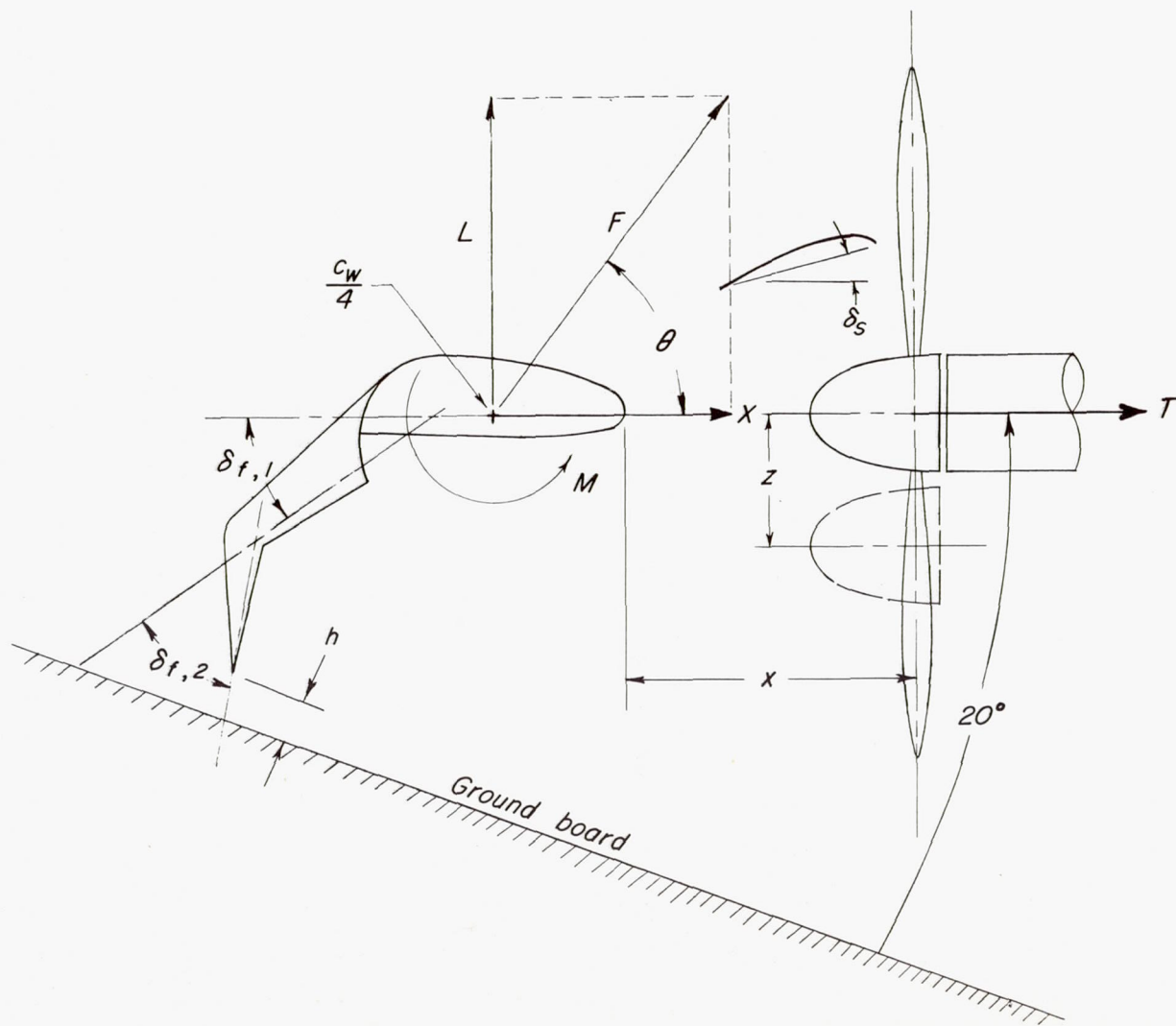
Figure 1.- Convention used to define positive sense of forces, moments, and angles.

Full-span nozzle at .38c_w

Plenum chamber

.15c_w

.038c_w

.35c_w

$c_w = 18.0$

.25c_w
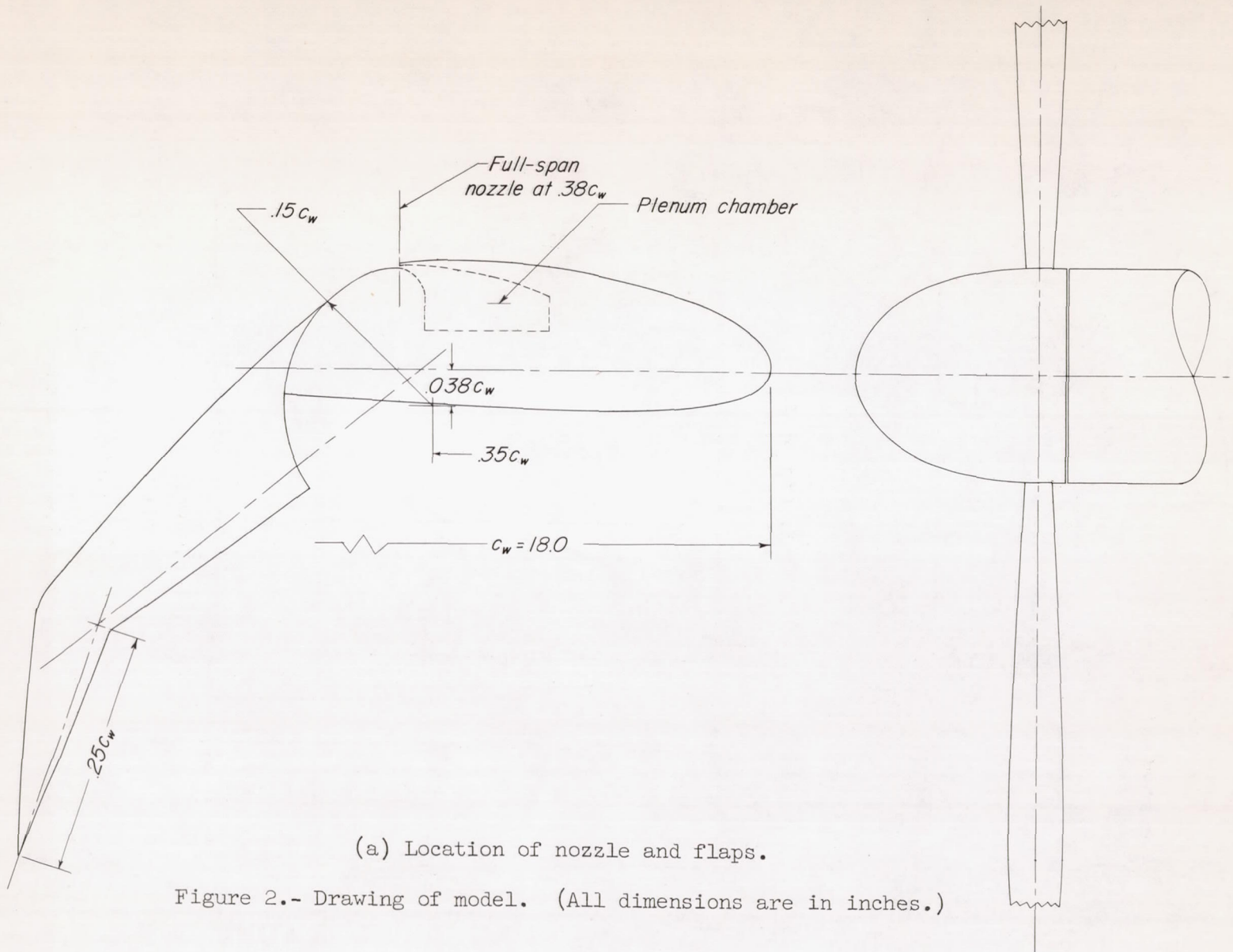
(a) Location of nozzle and flaps.

Figure 2.- Drawing of model. (All dimensions are in inches.)

$\frac{1}{16}$-in. sheet-metal
end plate

2.7

Saw cut

6.3

13.5

18

Section A-A

24

A

24

$12\frac{1}{4}$

A

Balance

$\frac{1}{8}$
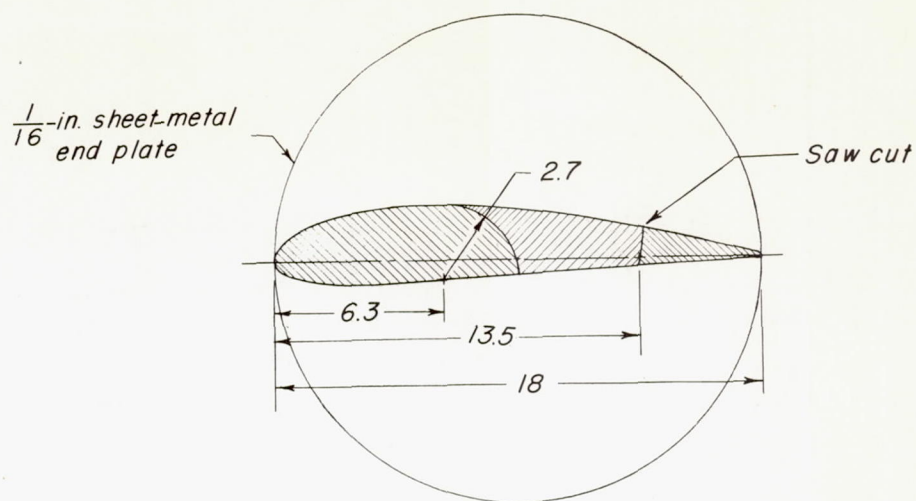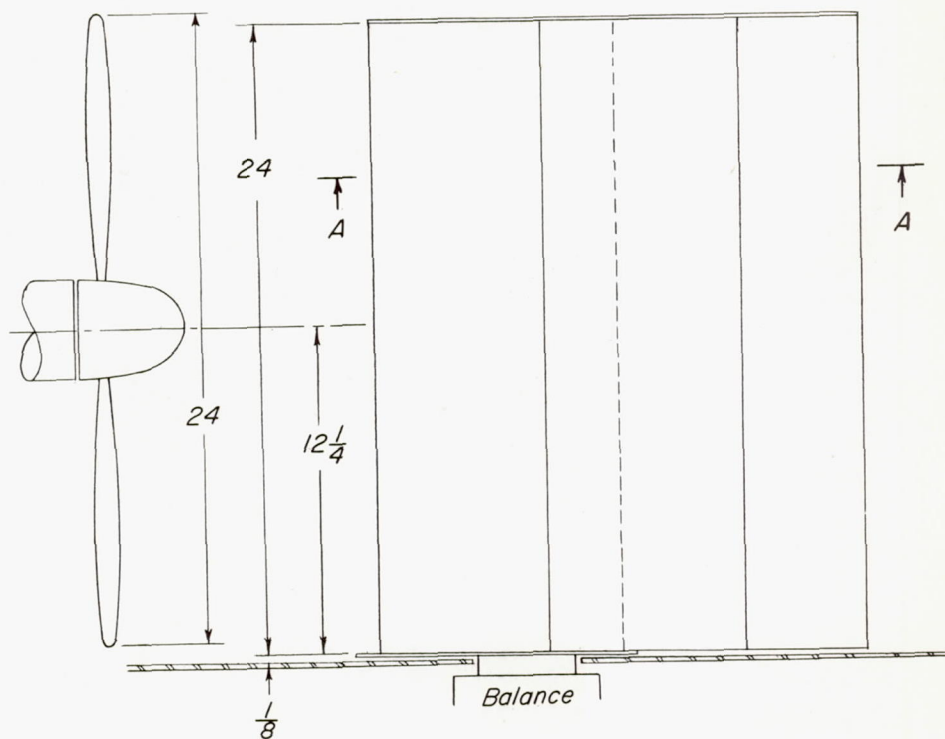
(b) End plate on.

Figure 2.- Concluded.
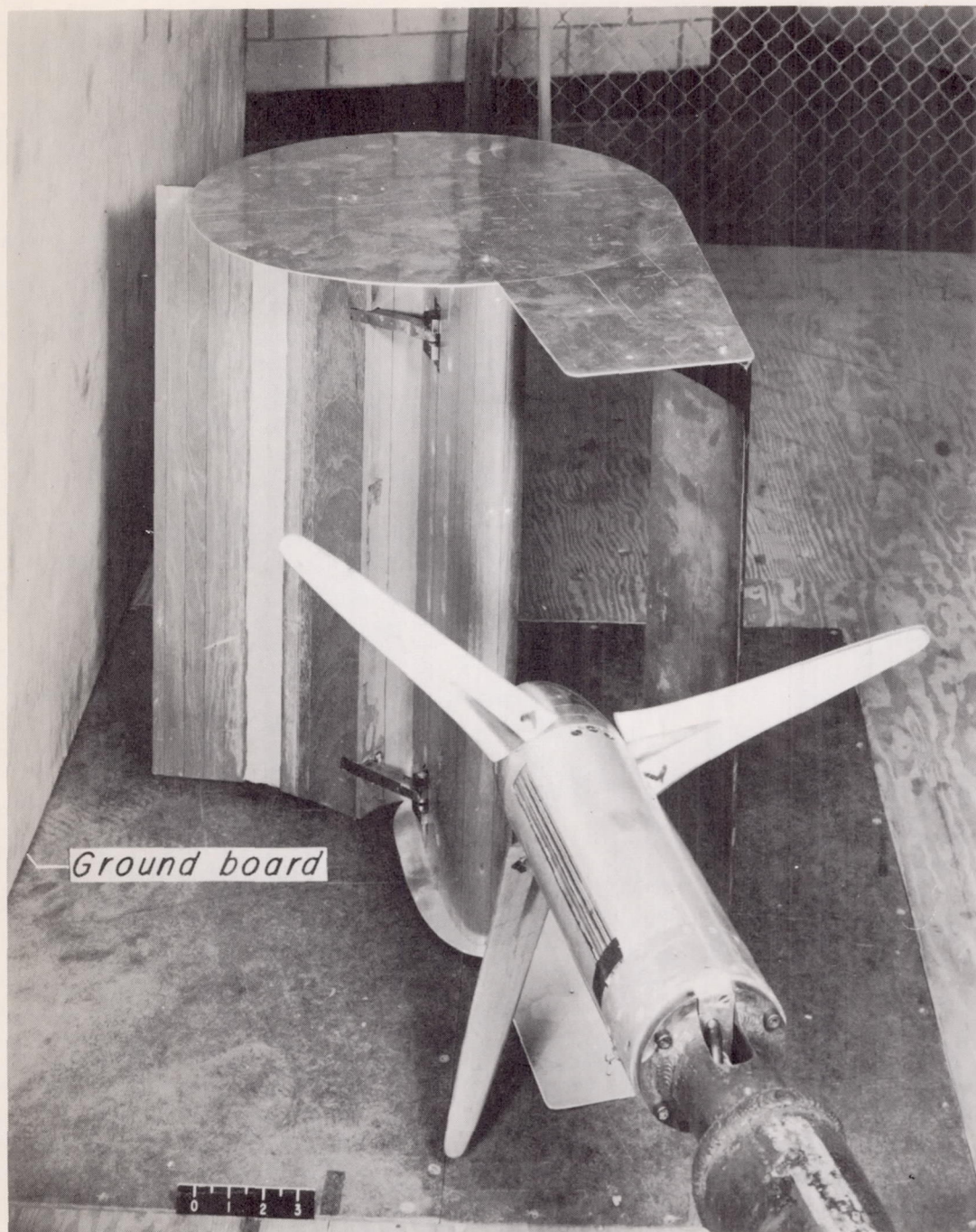
L-89993.2

Figure 3.- Model installed on static-thrust stand. End plate on; slat in
position B; ground board at $h/D \approx 0.1$.

$\frac{1}{16}$ - in. sheet-metal slat has contour
same as upper surface of forward
30 percent of wing chord

$\frac{1}{4}c_s$

δ_s

A

B

.17c_w

C

.11c_w

.17c_w .22c_w
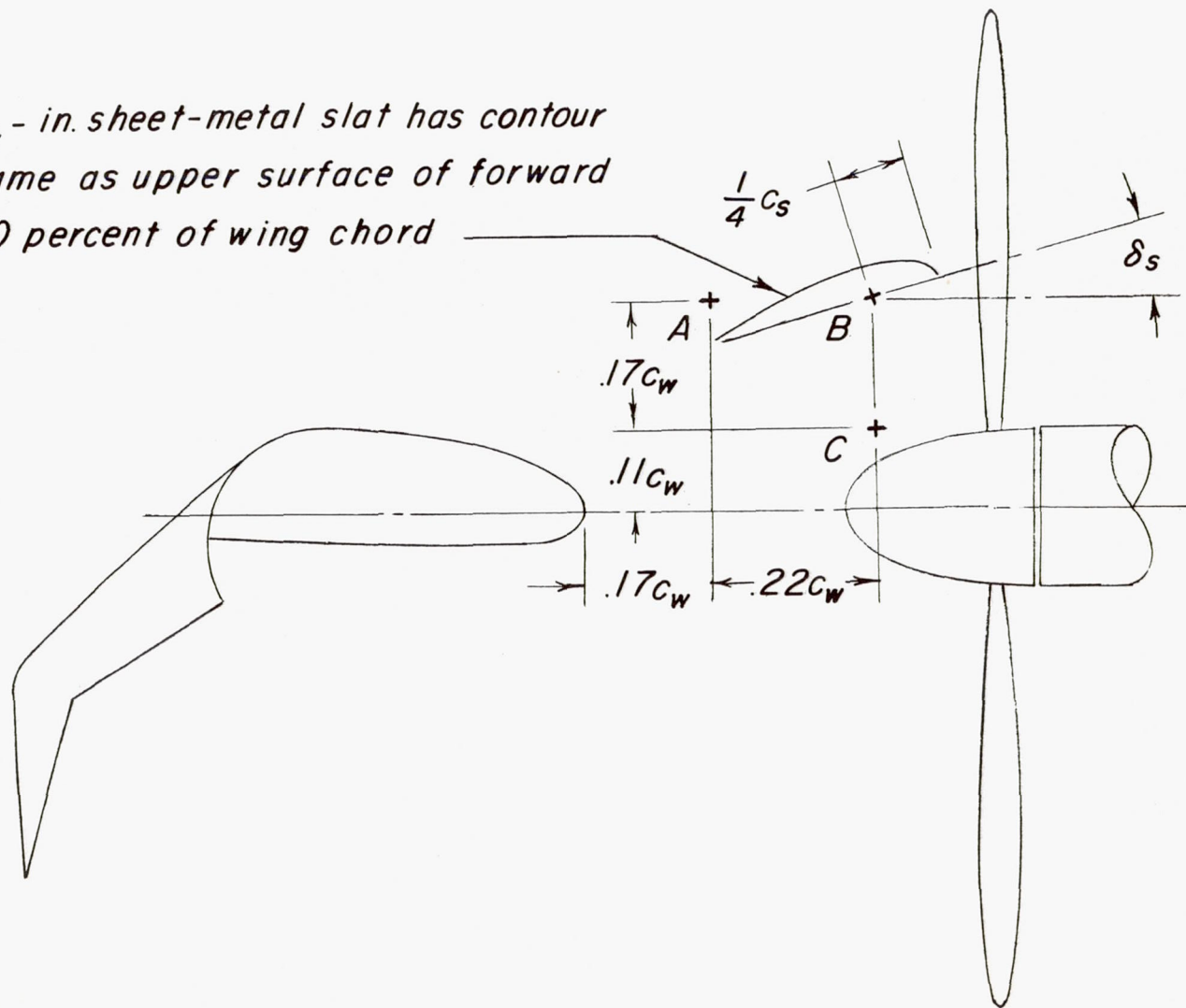
Figure 4.- Slat positions investigated.
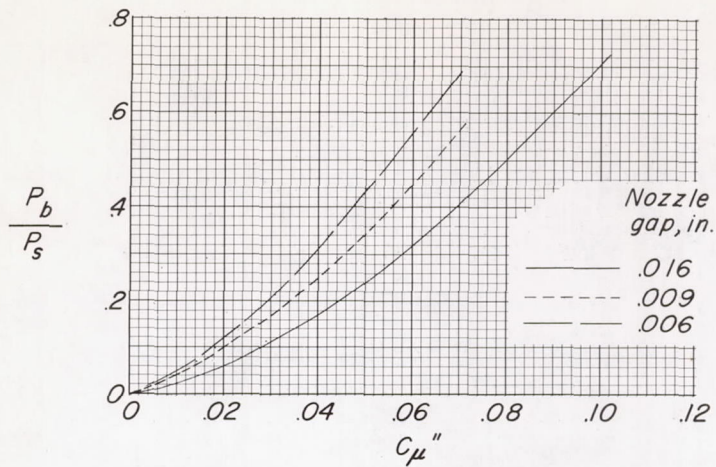
(a) Ratio of power in blowing system to power in slipstream.
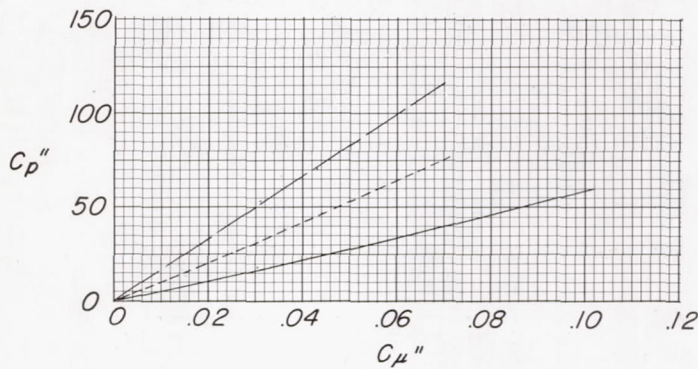
(b) Pressure coefficient.
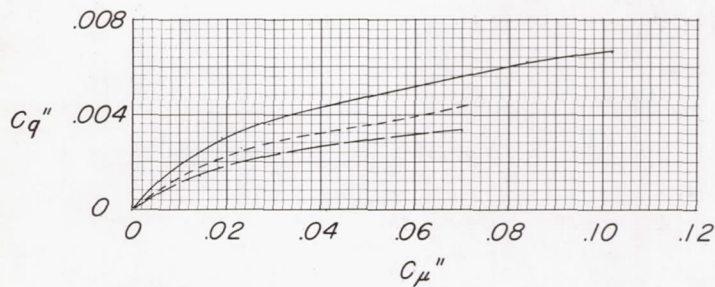
(c) Flow coefficient.

Figure 5.- Ratio of power in blowing system to power in slipstream, pressure coefficient, and flow coefficient against momentum coefficient for three nozzle gaps.
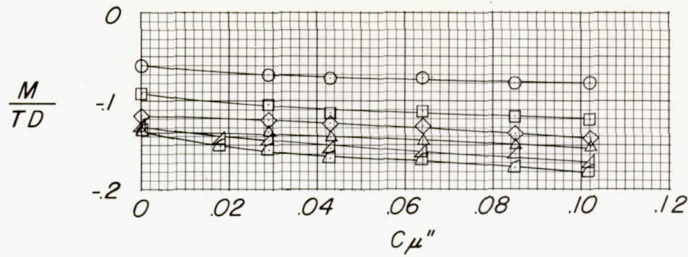
(a) Pitching moment.
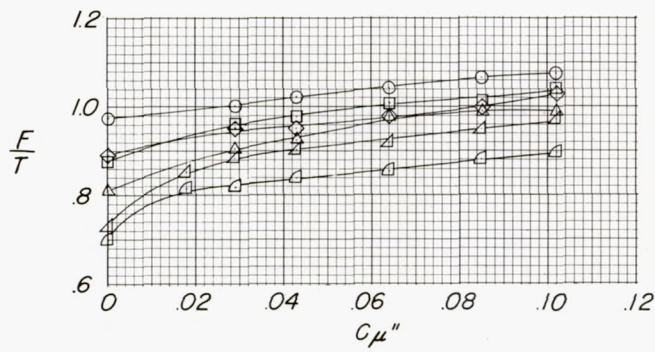
(b) Ratio of resultant force to thrust.
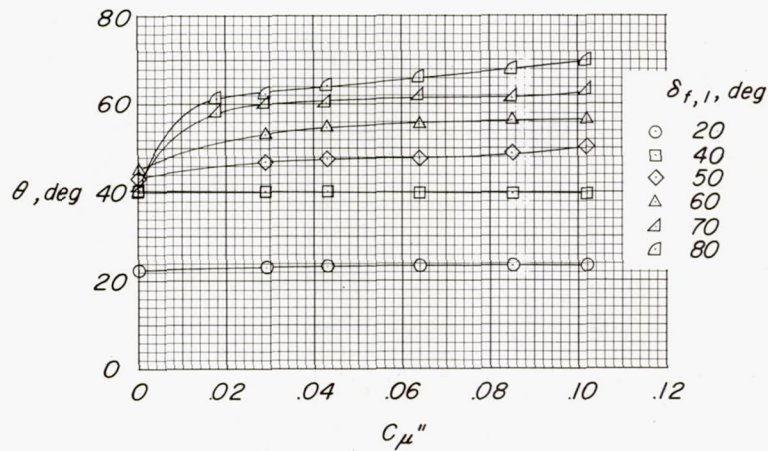
(c) Turning angle.

Figure 6.- Effect of blowing over the flap with $\delta_{f,2}$ constant at $0°$ on the characteristics of the model. $x/D = 0.41$; $z/D = 0$; $h/D = \infty$; nozzle gap, 0.016 inch.
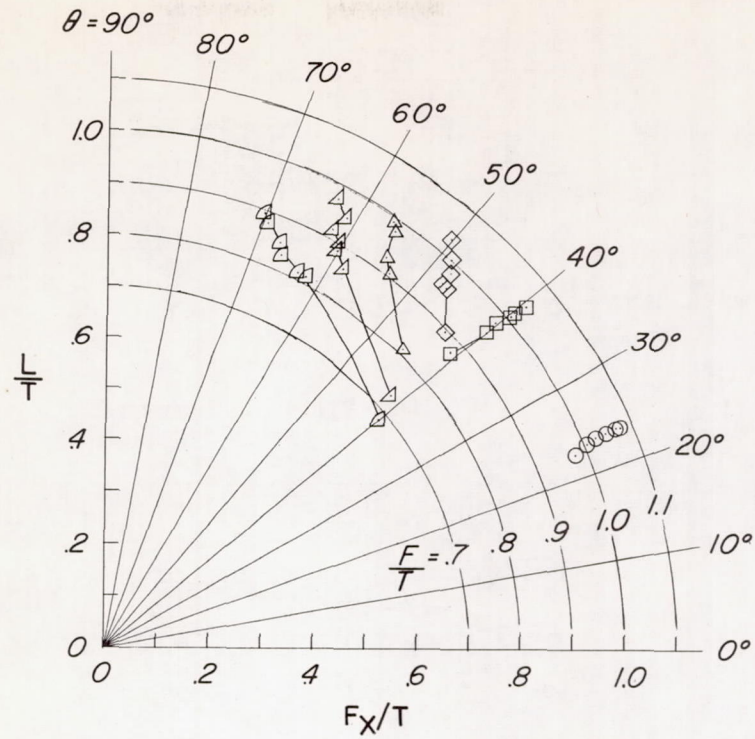
(d) Summary of turning effectiveness.
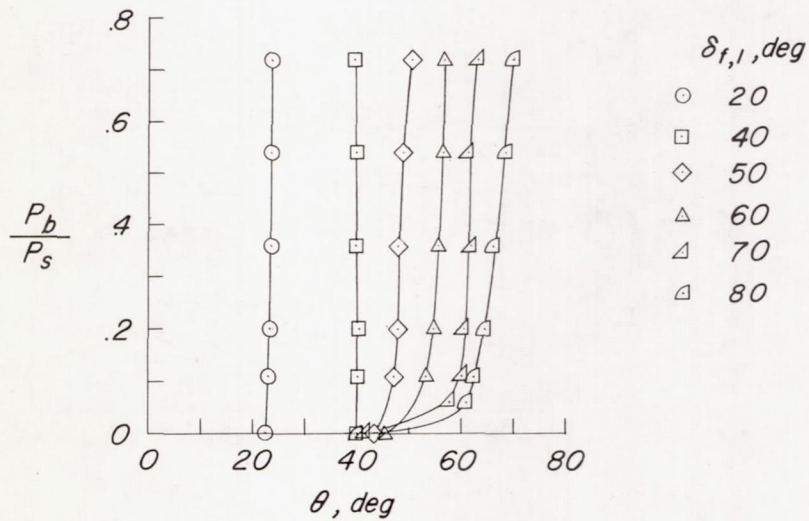
(e) Ratio of power in blowing system to power in slipstream against
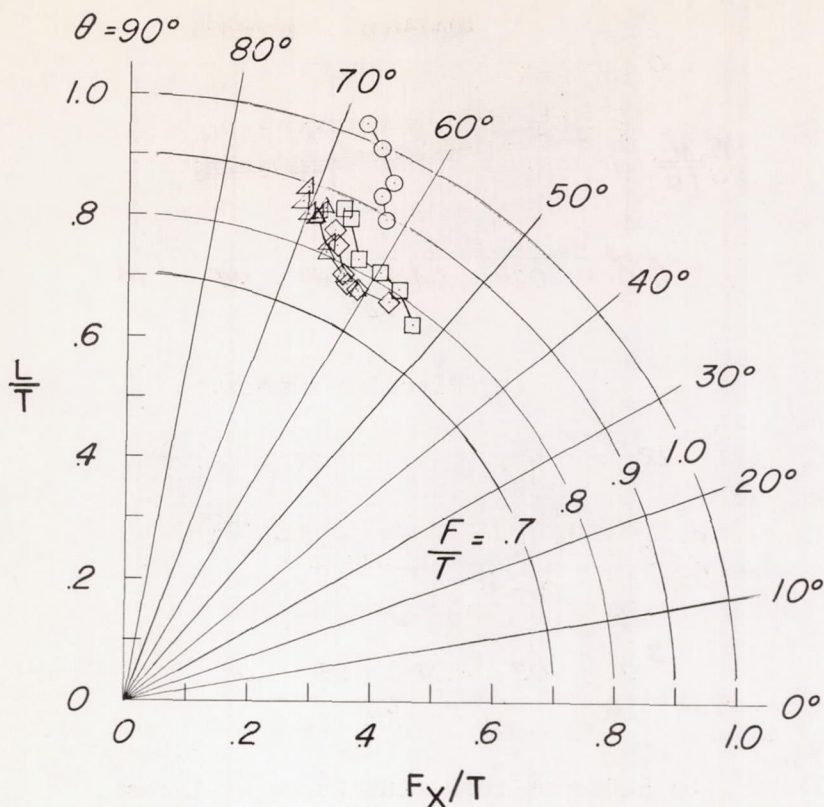turning angle.

Figure 6.- Concluded.
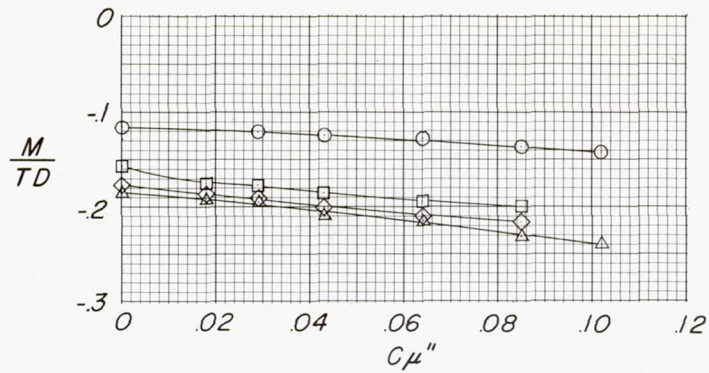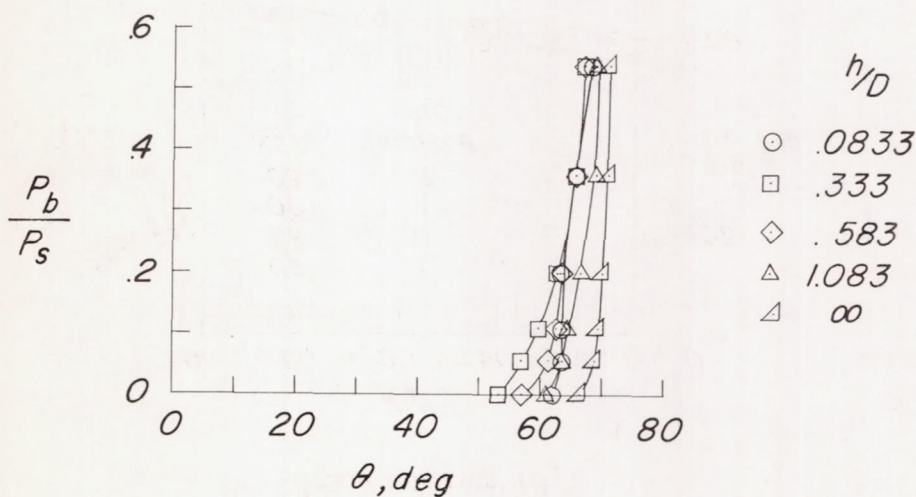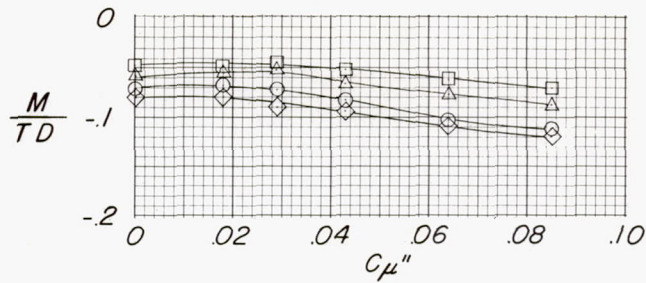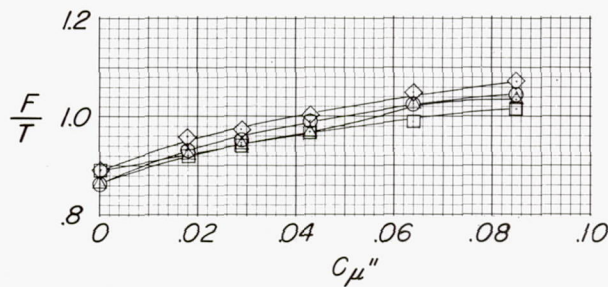
(a) Pitching moment.
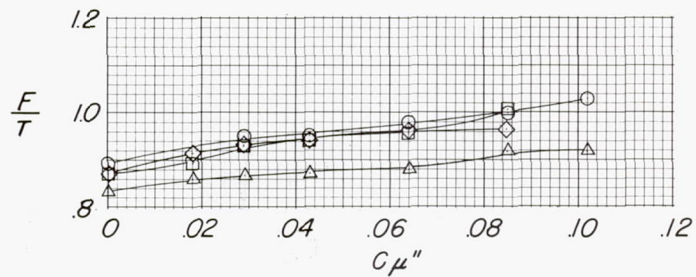
(b) Ratio of resultant force to thrust.
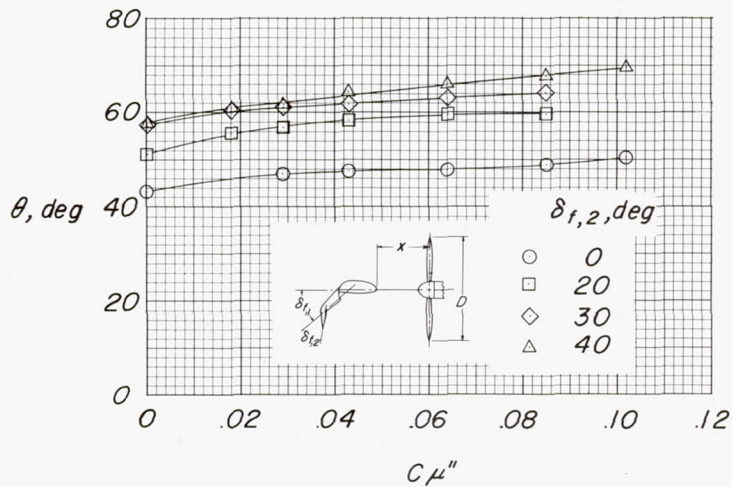
(c) Turning angle.

Figure 7.- Effect of blowing over the flap with $\delta_{f,1}$ constant at 50° on the characteristics of the model. $x/D = 0.41$; $z/D = 0$; $h/D = \infty$; nozzle gap, 0.016 inch.
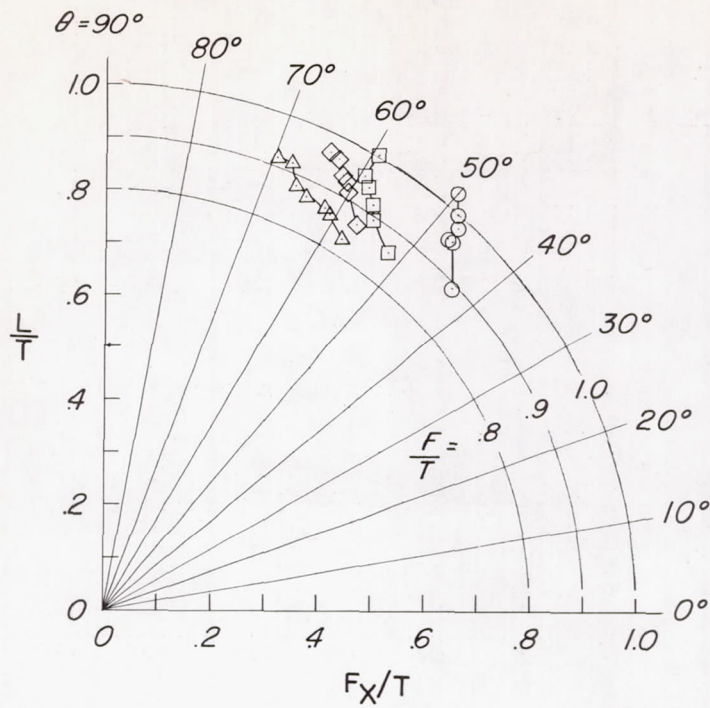
(d) Summary of turning effectiveness.
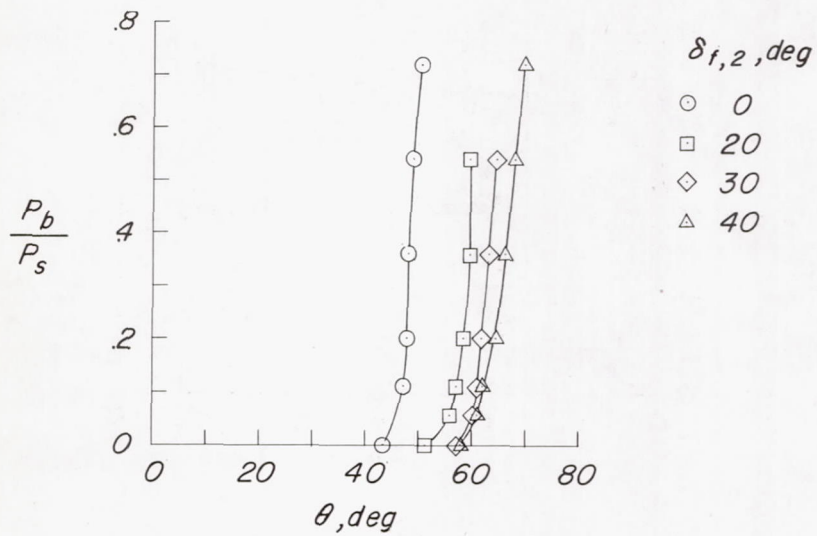
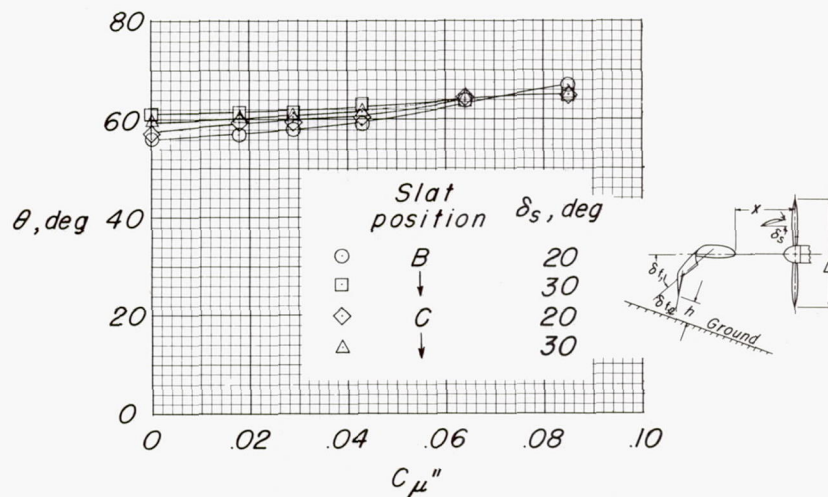(e) Ratio of power in blowing system to power in slipstream against turning angle.
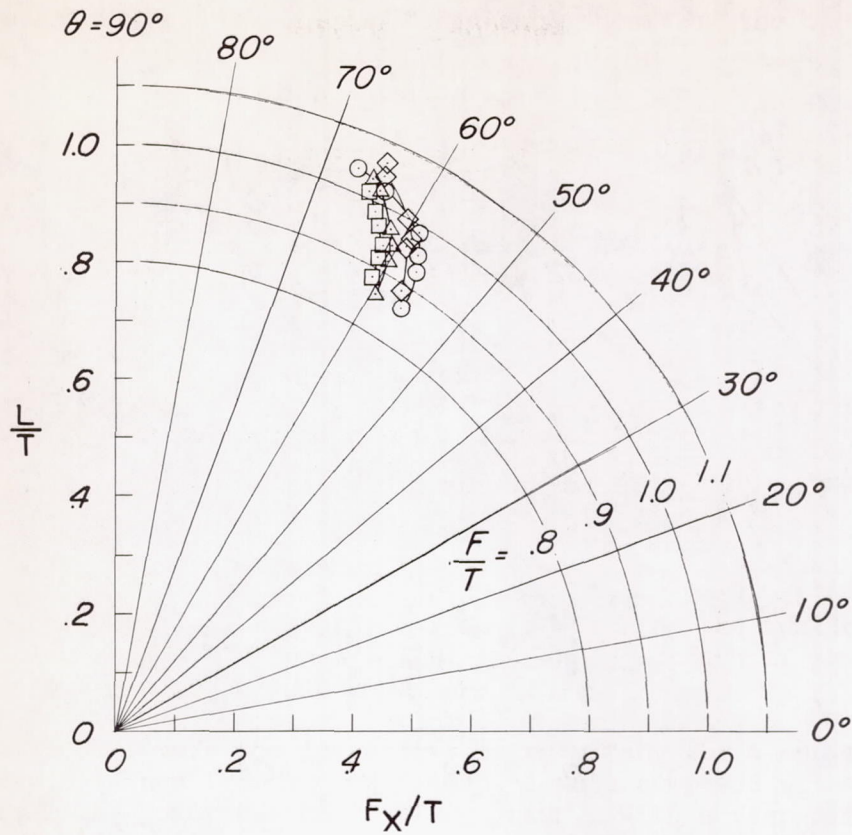
Figure 7.- Concluded.
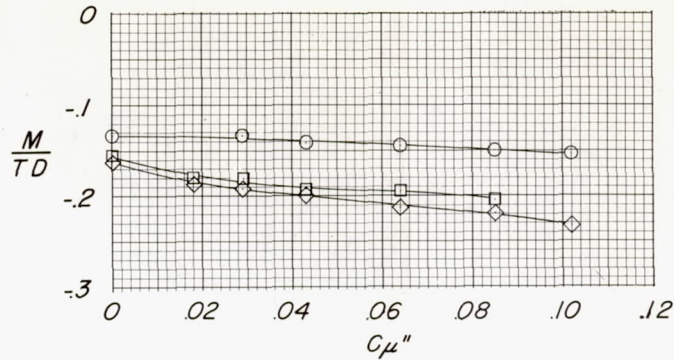
(a) Pitching moment.
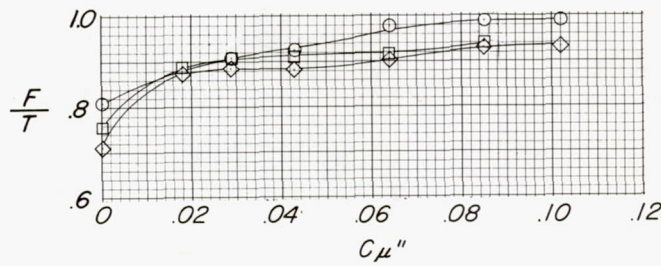
(b) Ratio of resultant force to thrust.
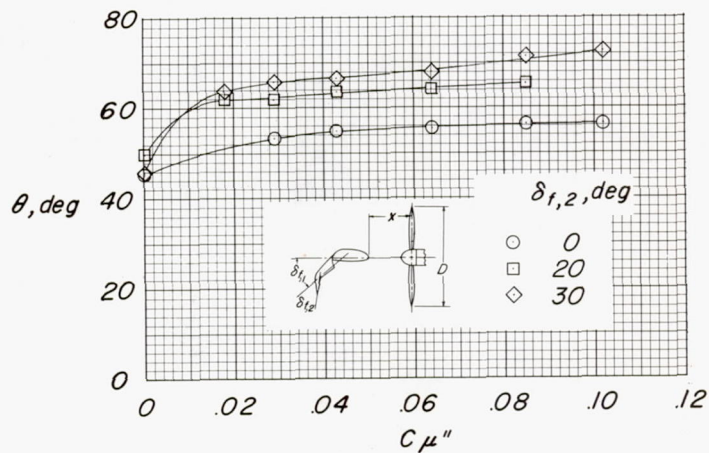
(c) Turning angle.

Figure 8.- Effect of blowing over the flap with $\delta_{f,1}$ constant at $60°$ on the characteristics of the model. $x/D = 0.41$; $z/D = 0$; $h/D = \infty$; nozzle gap, 0.016 inch.
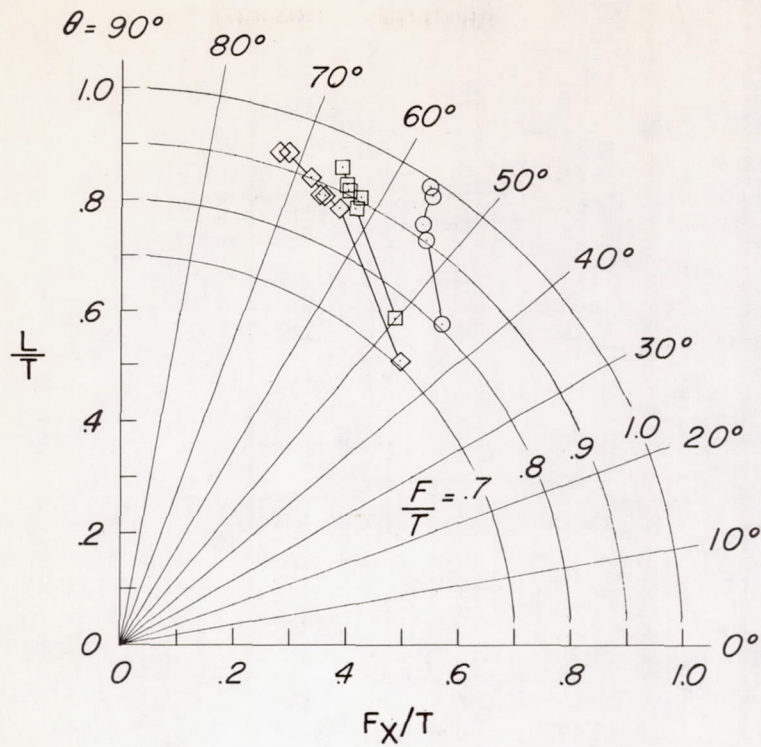
(d) Summary of turning effectiveness.
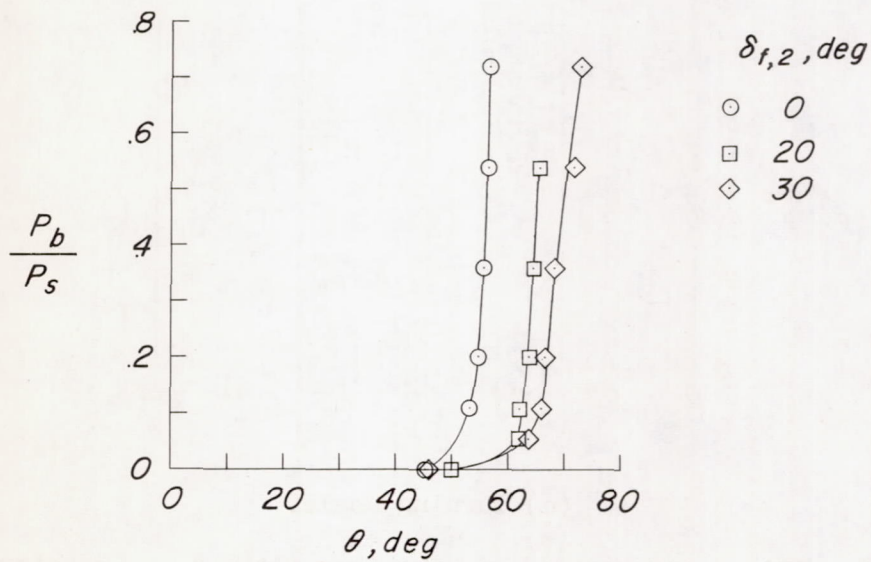
(e) Ratio of power in blowing system to power in slipstream against
turning angle.

Figure 8.- Concluded.
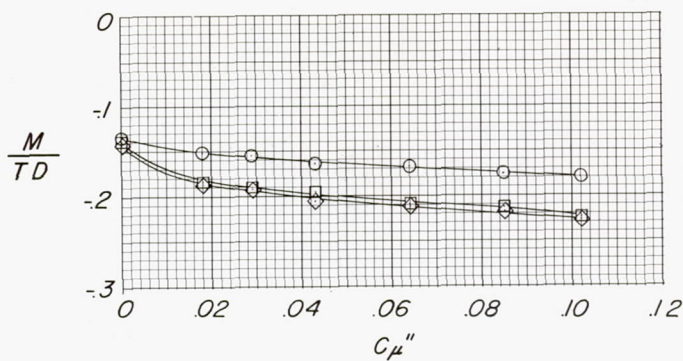
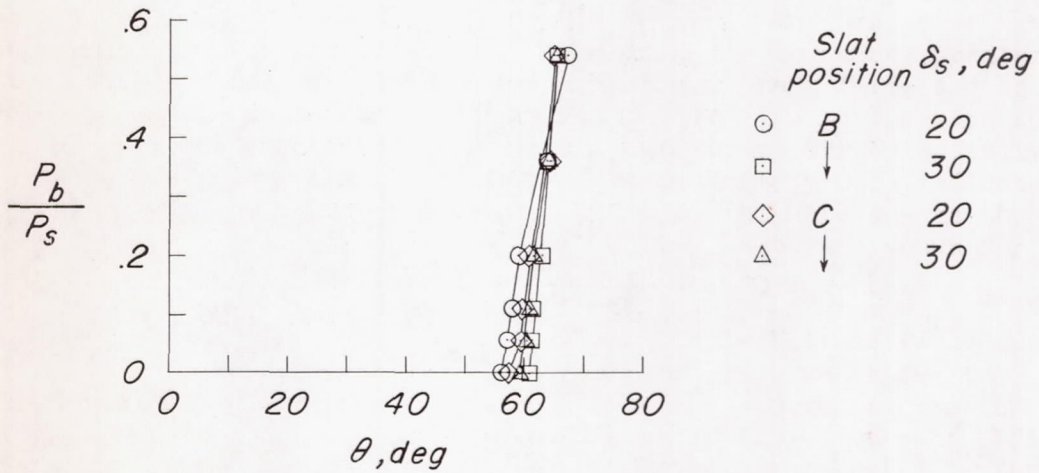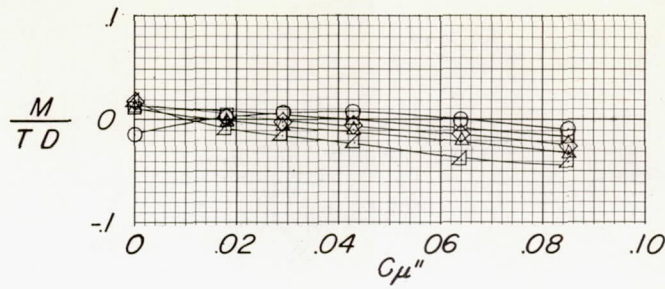(a) Pitching moment.
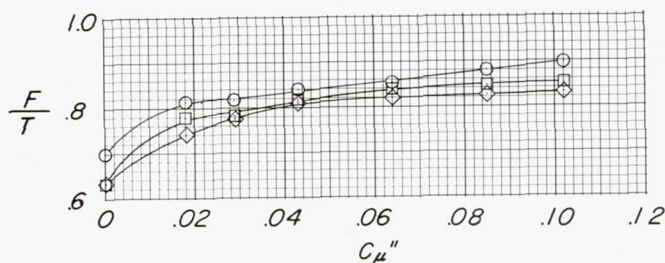
(b) Ratio of resultant force to thrust.
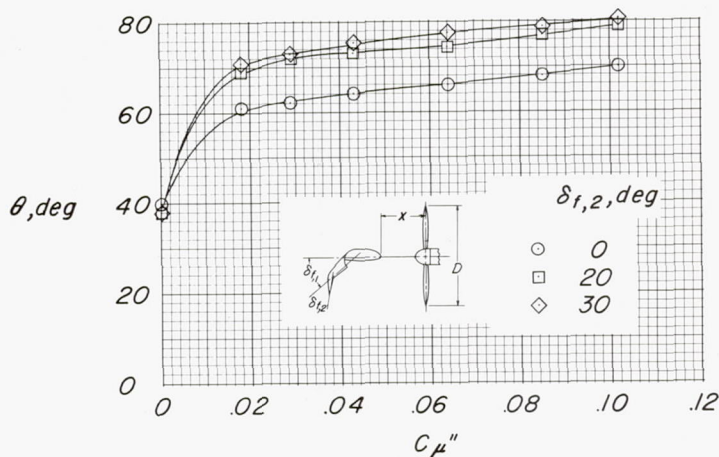
(c) Turning angle.

Figure 9.- Effect of blowing over the flap with $\delta_{f,1}$ constant at $80°$ on the characteristics of the model. $x/D = 0.41$; $z/D = 0$; $h/D = \infty$; nozzle gap, 0.016 inch.
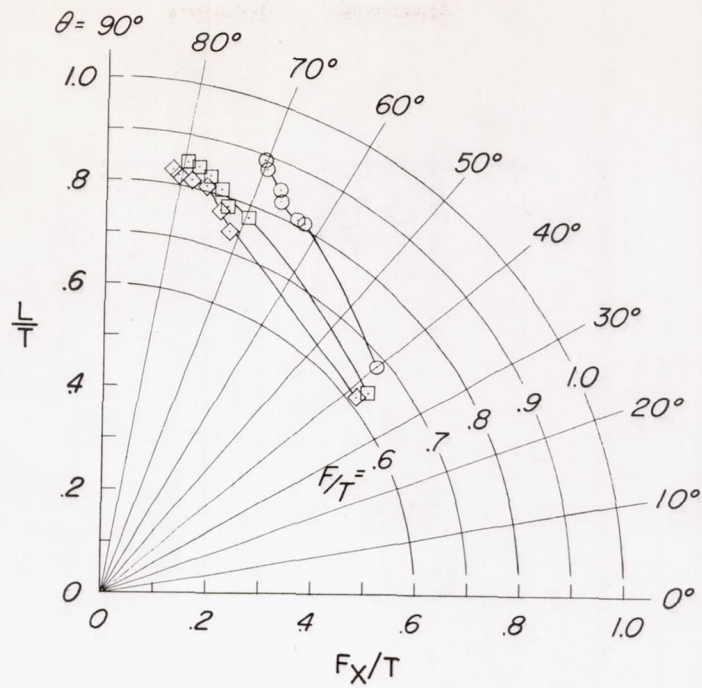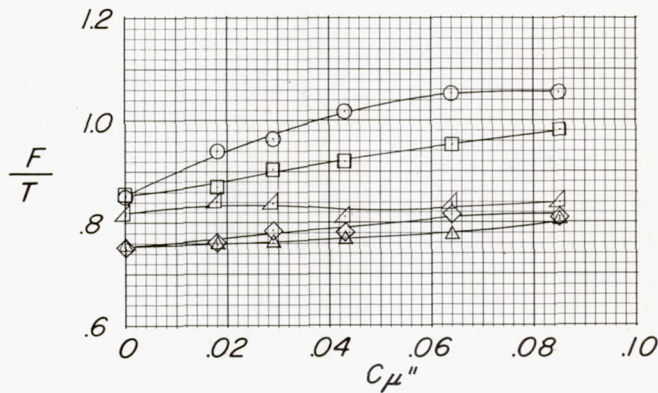
(d) Summary of turning effectiveness.
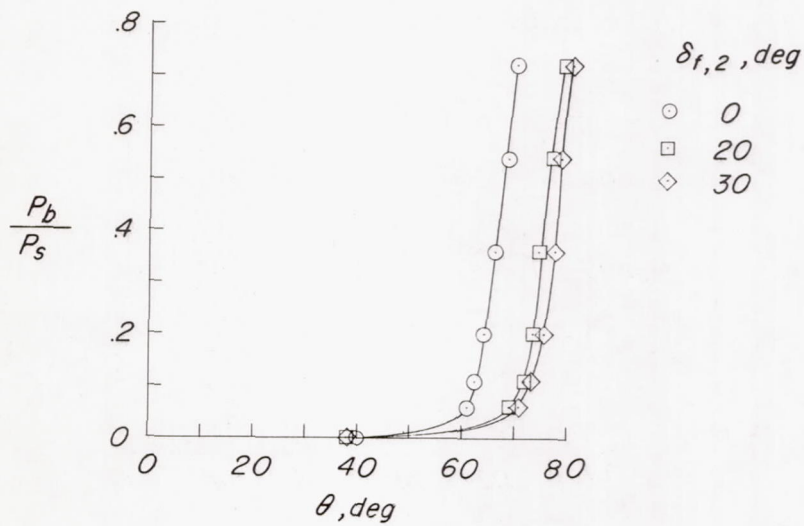
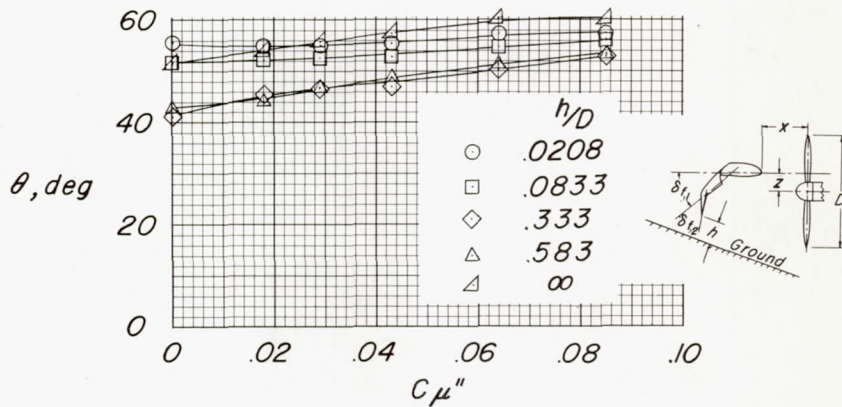(e) Ratio of power in blowing system to power in slipstream against turning angle.

Figure 9.- Concluded.
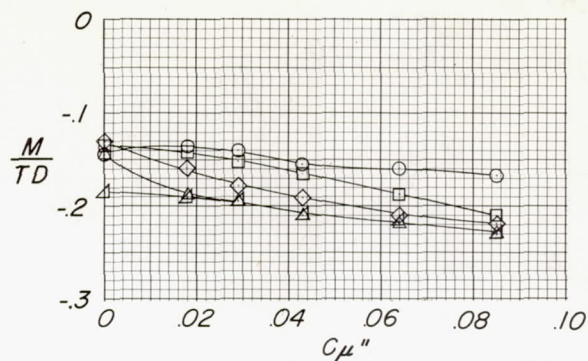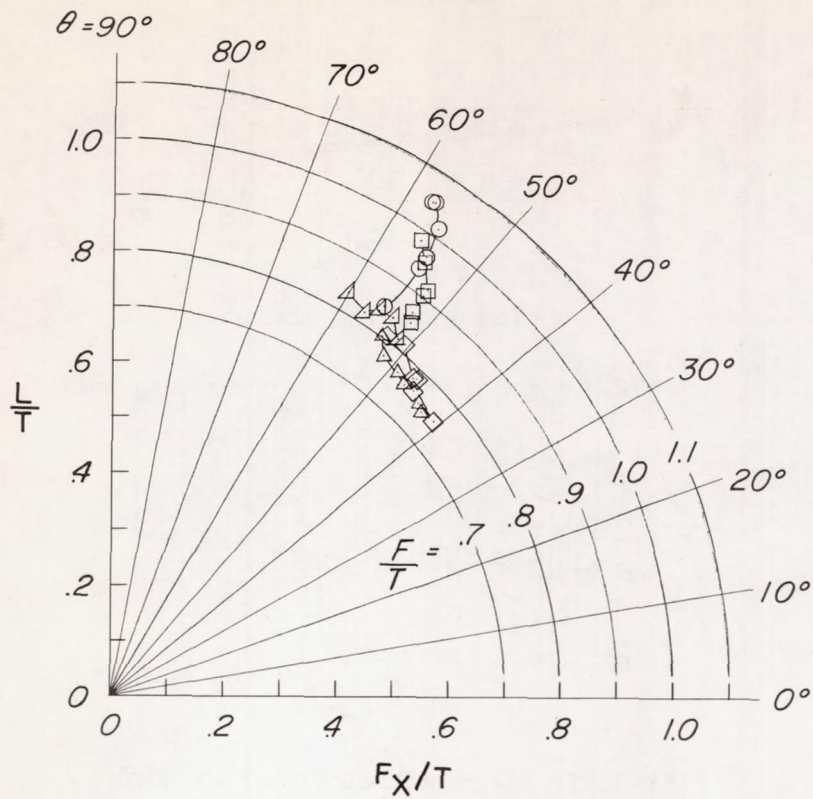
(a) Pitching moment.
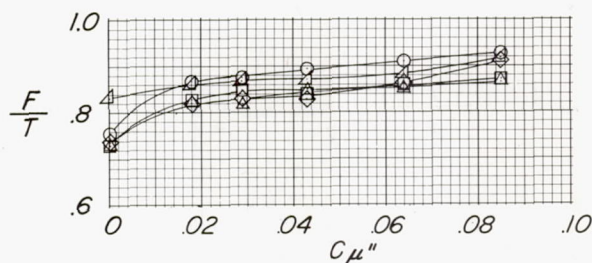
(b) Ratio of resultant force to thrust.
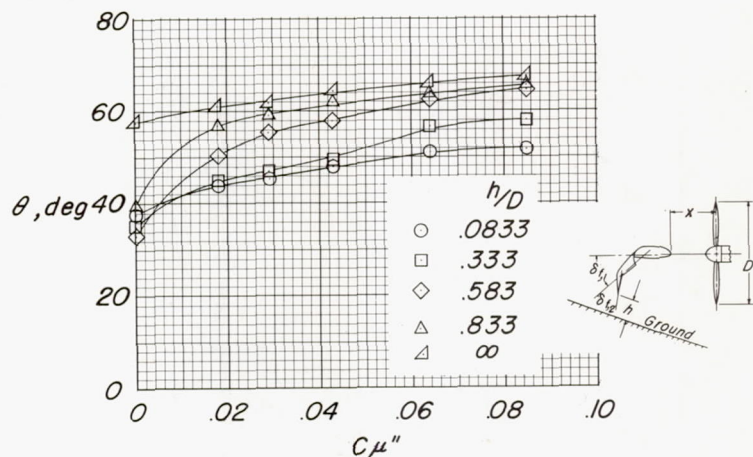
(c) Turning angle.

Figure 10.- Effect of height above the ground and blowing over the flap on the characteristics of the model. $\delta_{f,1} = 50°$; $\delta_{f,2} = 40°$; $x/D = 0.41$; $z/D = 0$; nozzle gap, 0.016 inch.
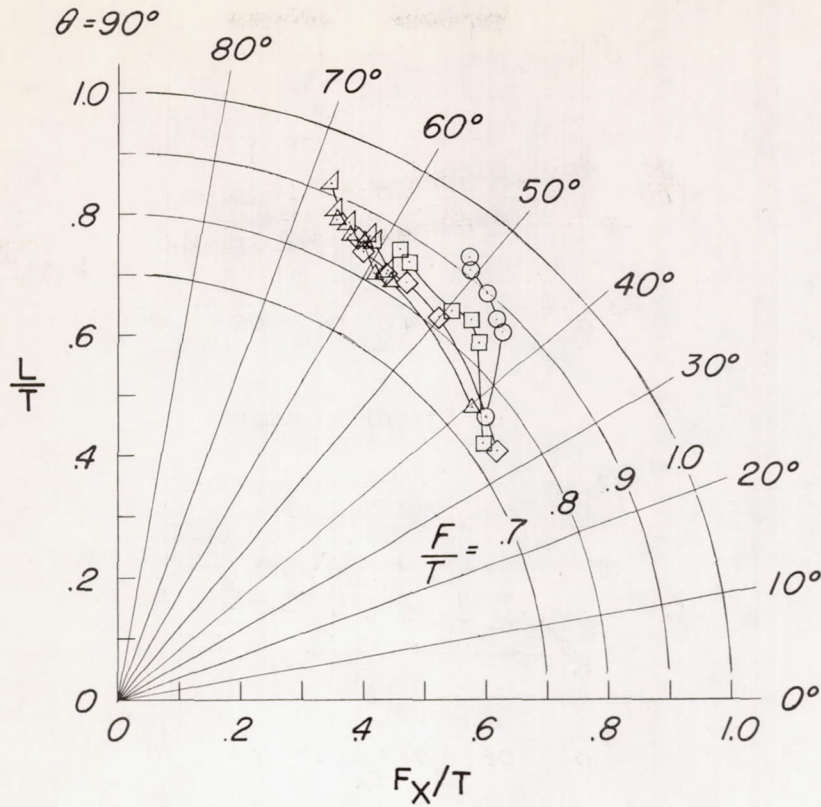
(d) Summary of turning effectiveness.
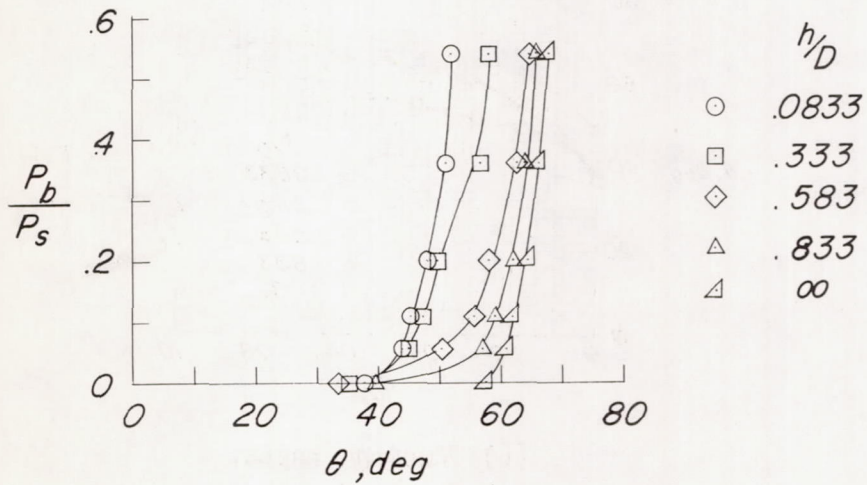
(e) Ratio of power in blowing system to power in slipstream against turning angle.

Figure 10.- Concluded.
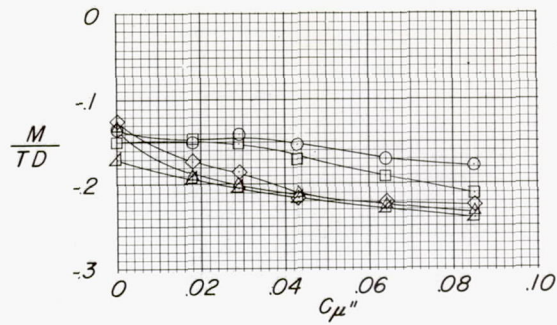
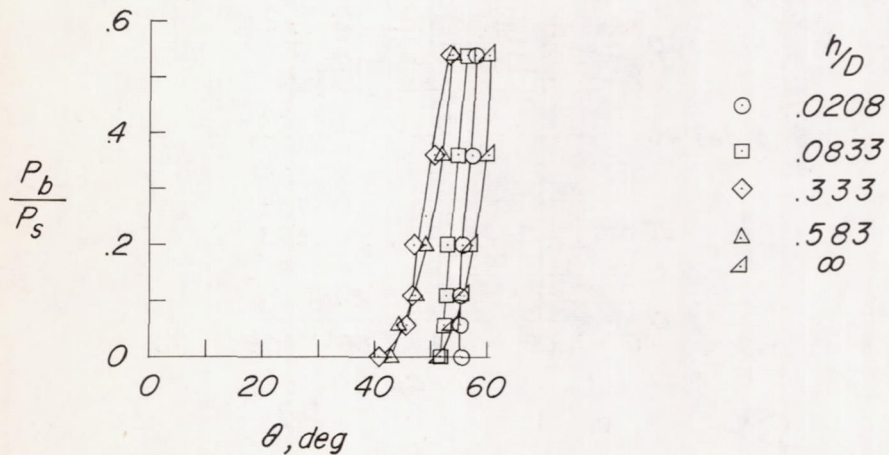(a) Pitching moment.
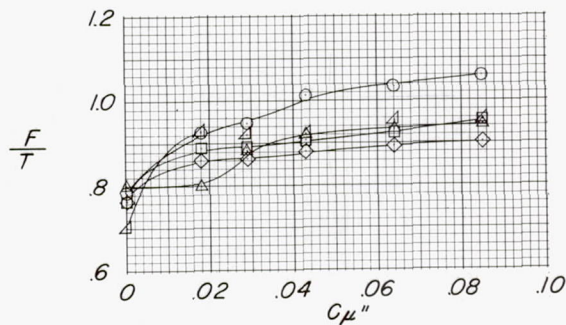
(b) Ratio of resultant force to thrust.
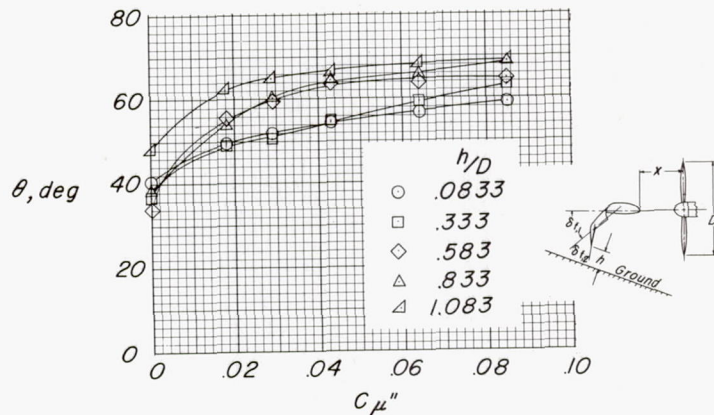
(c) Turning angle.

Figure 11.- Effect of height above the ground and blowing over the flap on the characteristics of the model with end plate on. $\delta_{f,1} = 50°$; $\delta_{f,2} = 40°$; $x/D = 0.41$; $z/D = 0$; nozzle gap, 0.016 inch.
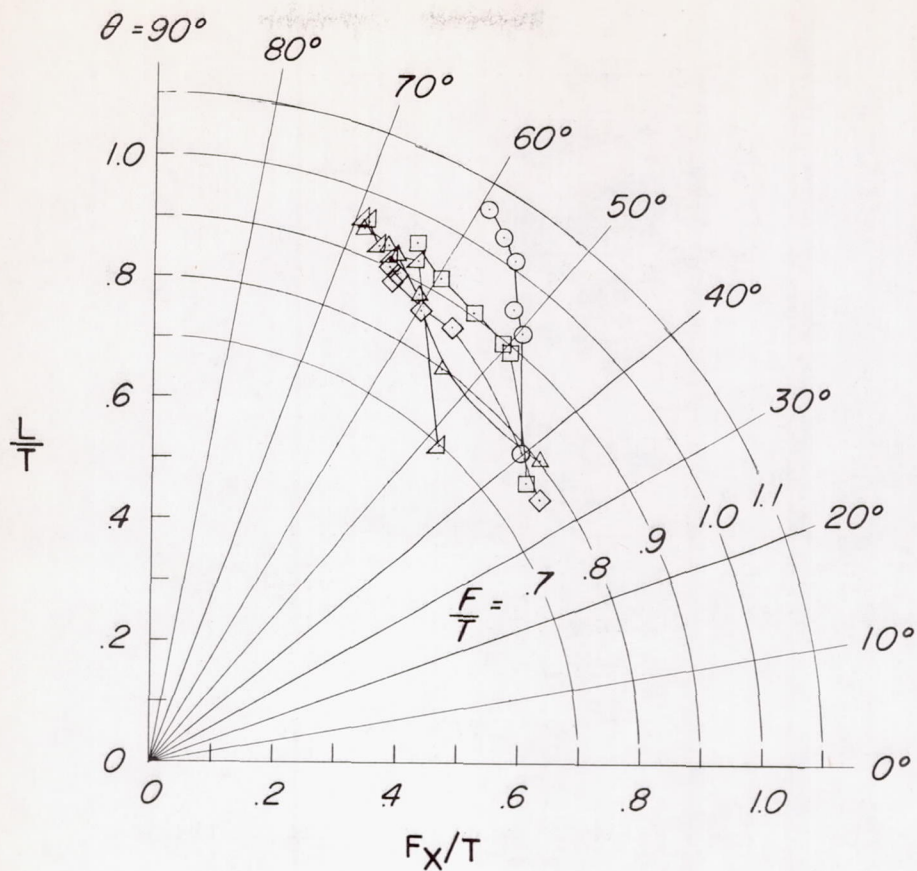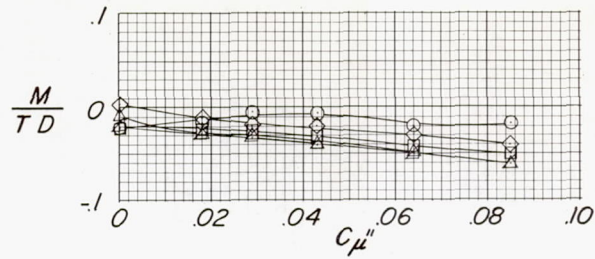
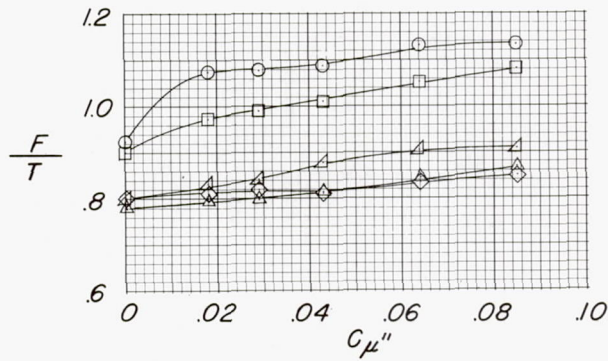(d) Summary of turning effectiveness.
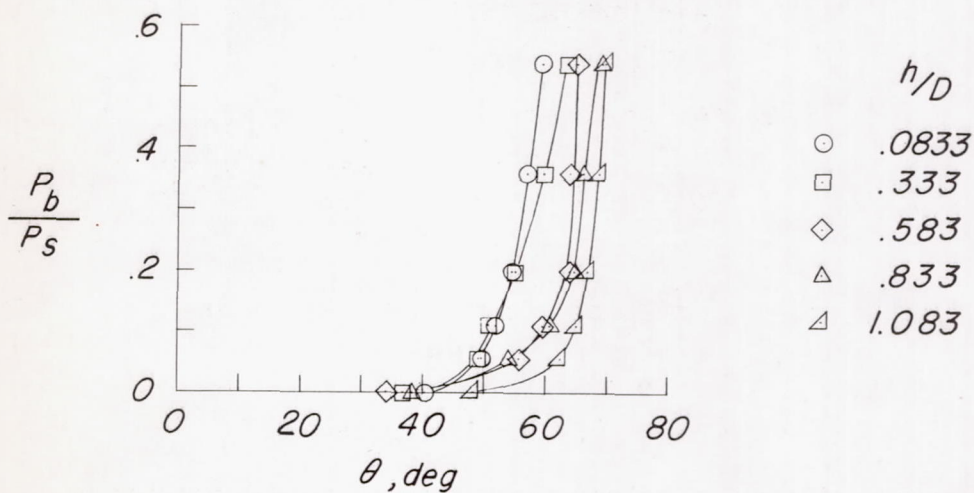
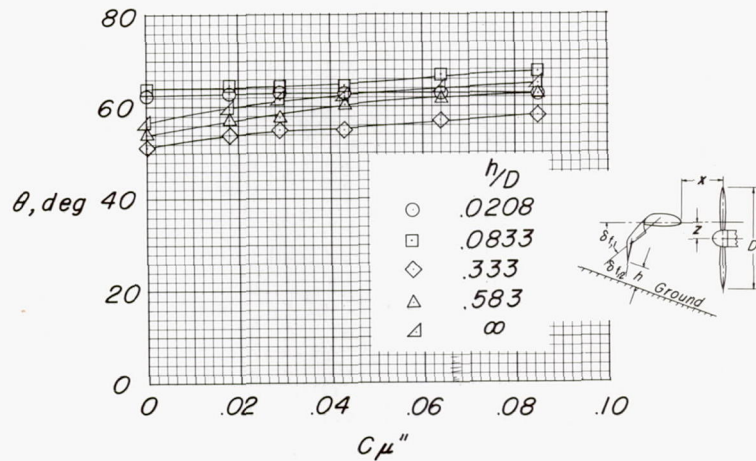(e) Ratio of power in blowing system to power in slipstream against turning angle.

Figure 11.- Concluded.
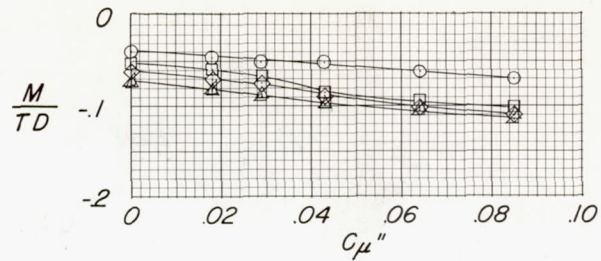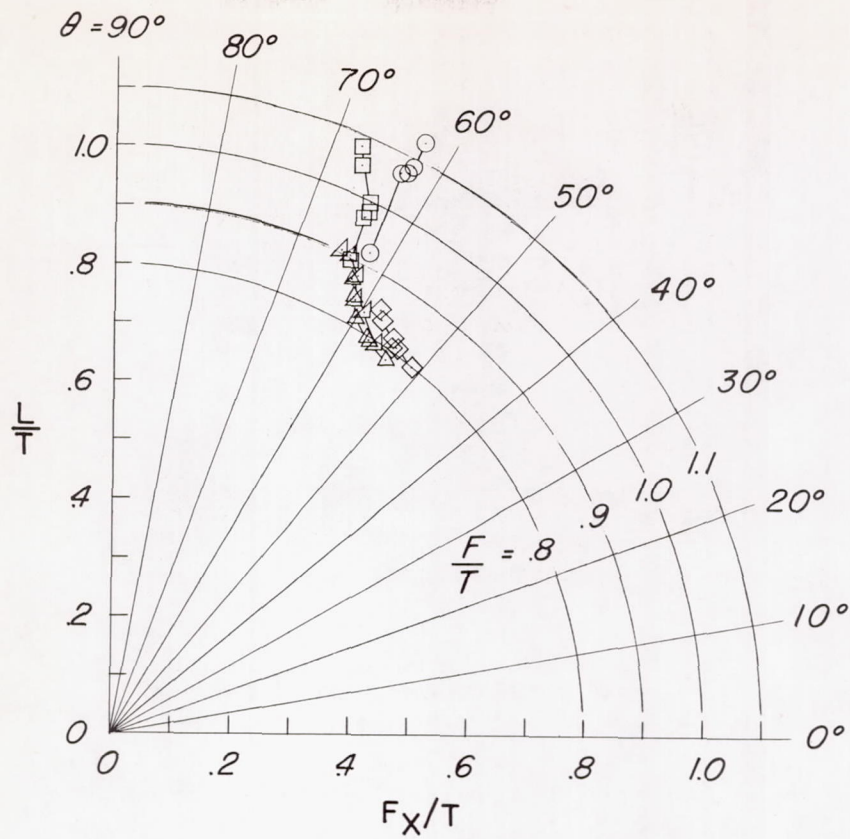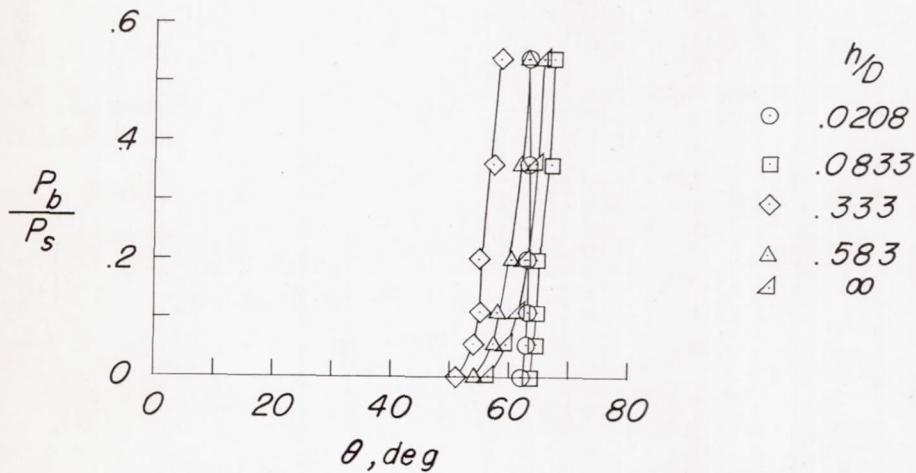
(a) Pitching moment.
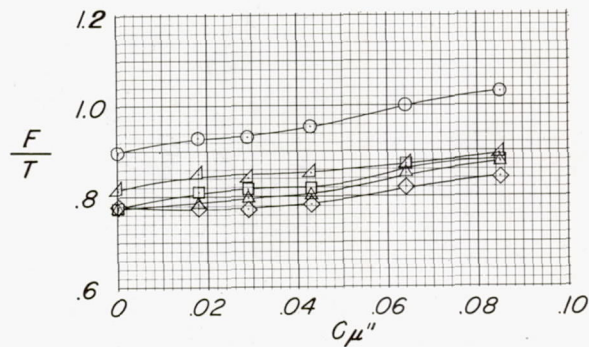
(b) Ratio of resultant force to thrust.
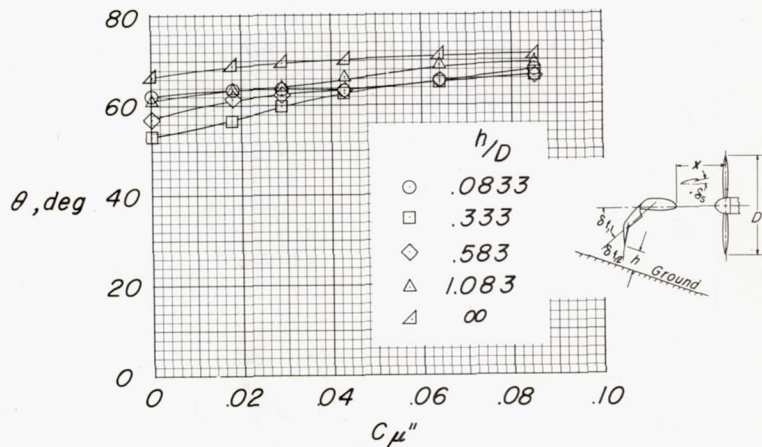
(c) Turning angle.

Figure 12.- Effect of height above the ground and blowing over the flap on the characteristics of the model with slat at position A and end plate on. $\delta_{f,1} = 50°$; $\delta_{f,2} = 40°$; $\delta_s = 30°$; $x/D = 0.41$; $z/D = 0$; nozzle gap, 0.016 inch.

(d) Summary of turning effectiveness.

(e) Ratio of power in blowing system to power in slipstream against turning angle.

Figure 12.- Concluded.

(a) Pitching moment.

(b) Ratio of resultant force to thrust.

(c) Turning angle.

Figure 13.- Effect of slat position, slat angle, and blowing over the flap
on the characteristics of the model. $\delta_{f,1} = 50^\circ$; $\delta_{f,2} = 40^\circ$; $x/D = 0.41$;
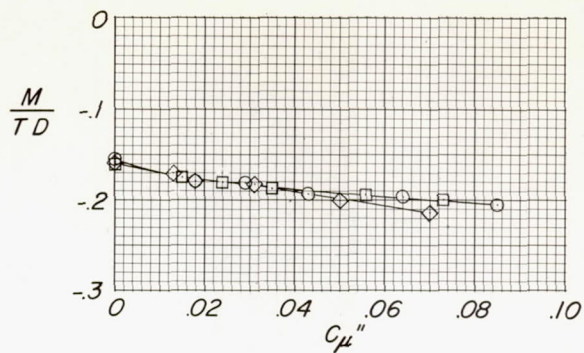$z/D = 0$; $h/D = 0.0833$; nozzle gap, 0.016 inch.

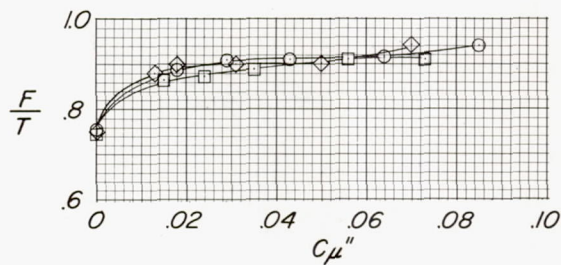(d) Summary of turning effectiveness.

(e) Ratio of power in blowing system to power in slipstream against turning angle.

Figure 13.- Concluded.

(a) Pitching moment.

(b) Ratio of resultant force to thrust.

(c) Turning angle.

Figure 14.- Effect of height above the ground and blowing over the flap
on the characteristics of the model. $\delta_{f,1} = 50^\circ$; $\delta_{f,2} = 40^\circ$; $x/D = 0.167$;
$z/D = 0.167$; nozzle gap, 0.016 inch.

(d) Summary of turning effectiveness.

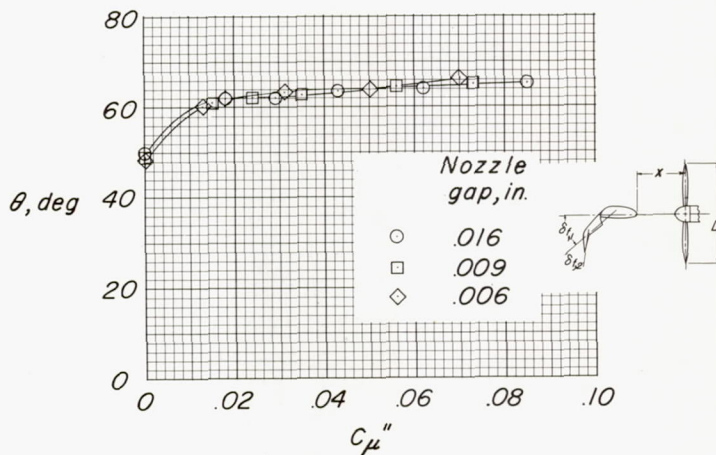(e) Ratio of power in blowing system to power in slipstream against turning angle.

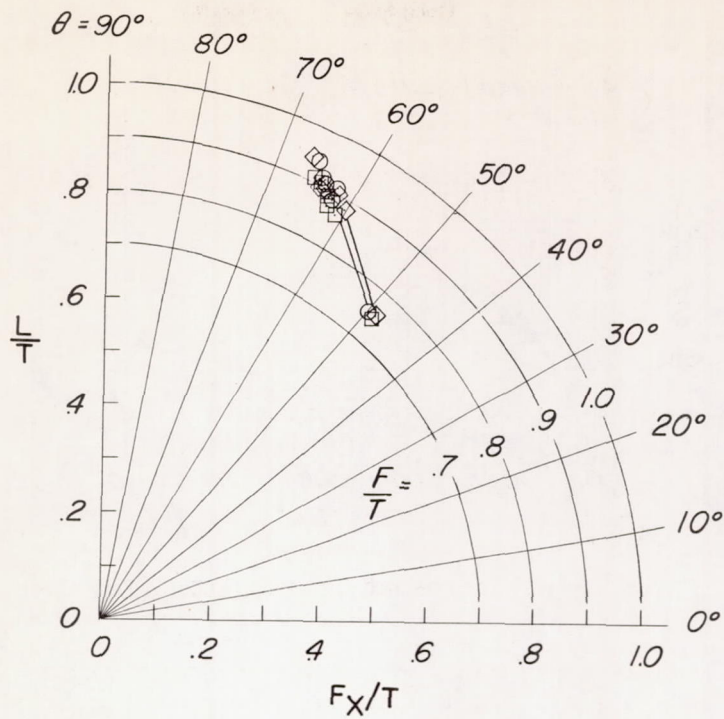Figure 14.- Concluded.

(a) Pitching moment.

(b) Ratio of resultant force to thrust.

(c) Turning angle.

Figure 15.- Effect of height above the ground and blowing over the flap on the characteristics of the model with end plate on. $\delta_{f,1} = 50°$; $\delta_{f,2} = 40°$; $x/D = 0.167$; $z/D = 0.167$; nozzle gap, 0.016 inch.

(d) Summary of turning effectiveness.

(e) Ratio of power in blowing system to power in slipstream against turning angle.

Figure 15.- Concluded.

(a) Pitching moment.

(b) Ratio of resultant force to thrust.

(c) Turning angle.

Figure 16.- Effect of nozzle gap and blowing over the flap on the charac-
teristics of the model. $\delta_{f,1} = 60°$; $\delta_{f,2} = 20°$; x/D = 0.41; z/D = 0;
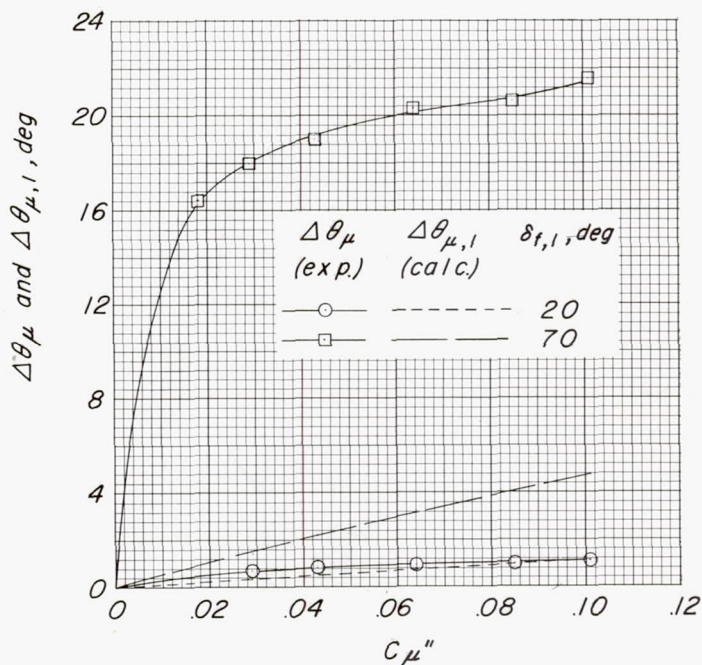h/D = ∞.

(d) Summary of turning effectiveness.
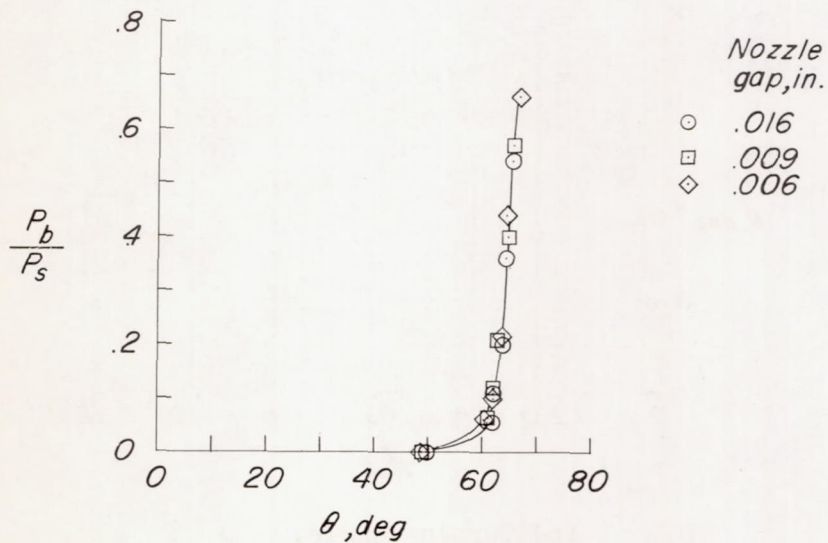
(e) Ratio of power in blowing system to power in slipstream against
turning angle.
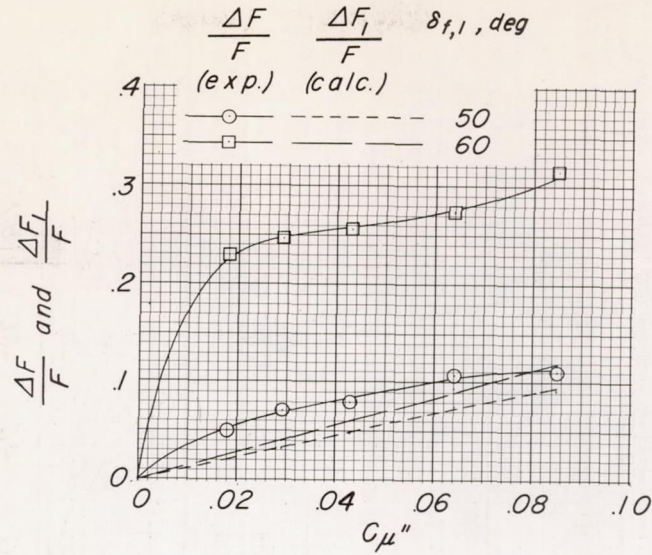
Figure 16.- Concluded.
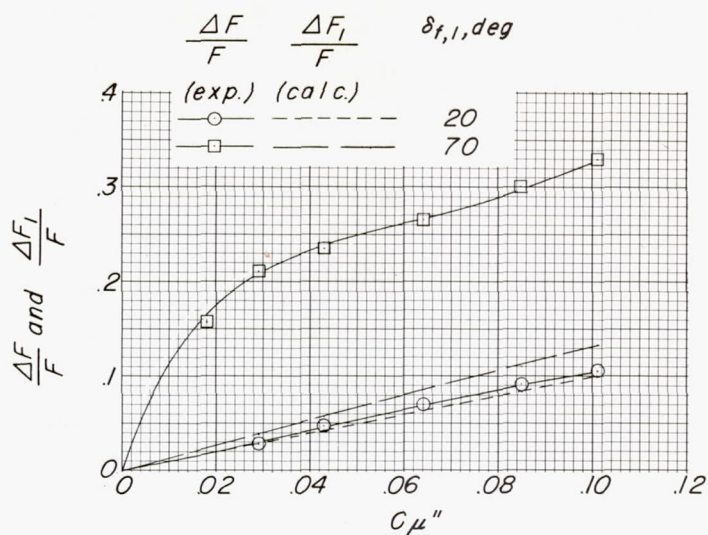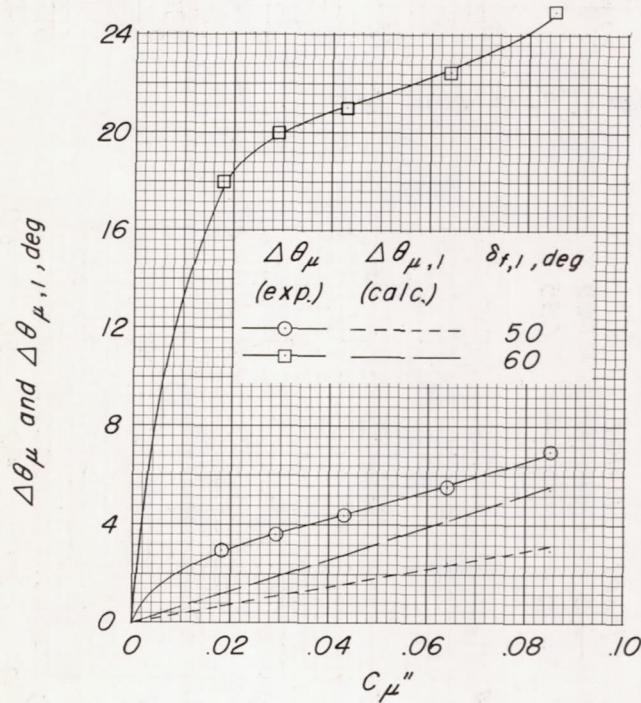
(a) Increment in resultant force.

(b) Increment in turning angle.

Figure 17.- Comparison of calculated and experimental increments in
resultant force and turning angle due to blowing over the flap.
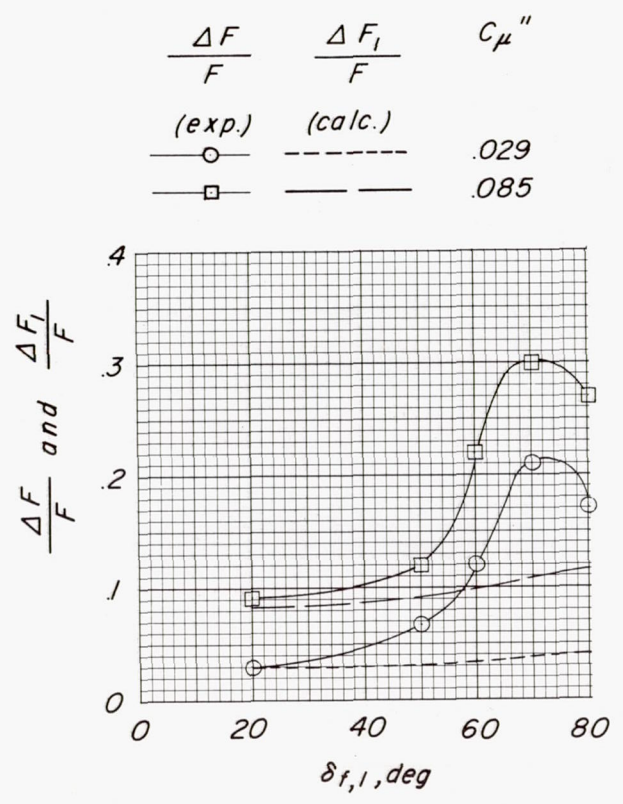$\delta_{f,2} = 0°$; $x/D = 0.41$; $z/D = 0$; $h/D = \infty$; nozzle gap, 0.016 inch.

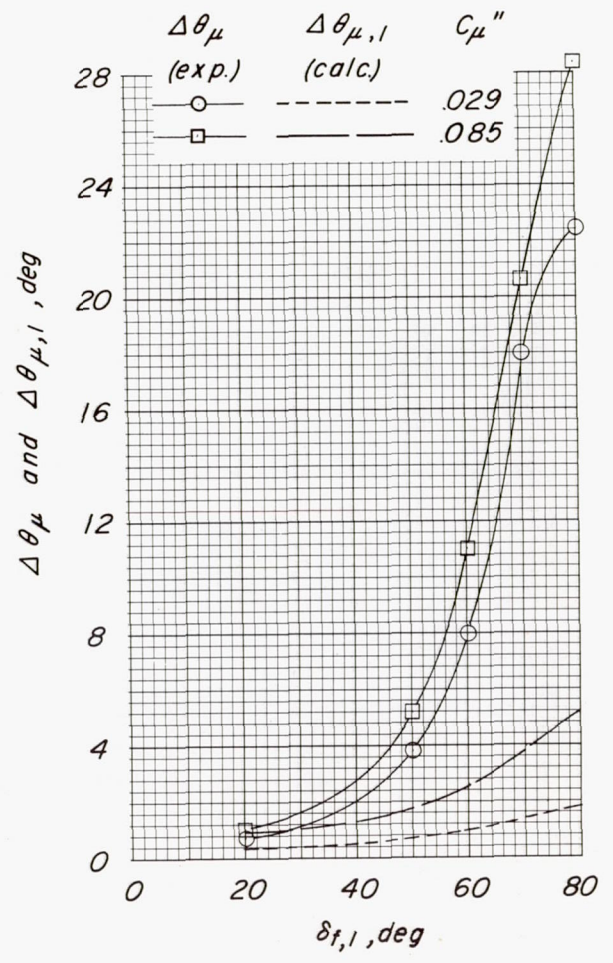(a) Increment in resultant force.

(b) Increment in turning angle.

Figure 18.- Comparison of calculated and experimental increments in resultant force and turning angle due to blowing over the flap. $\delta_{f,2} = 30^\circ$; $x/D = 0.41$; $z/D = 0$; $h/D = \infty$; nozzle gap, 0.016 inch.

(a) Increment in resultant force.

(b) Increment in turning angle.

Figure 19.- Comparison of calculated and experimental increments in resultant force and turning angle with changes in flap angle due to blowing over the flap. $\delta_{f,2} = 0°$; $x/D = 0.41$; $z/D = 0$; $h/D = \infty$; nozzle gap, 0.016 inch.
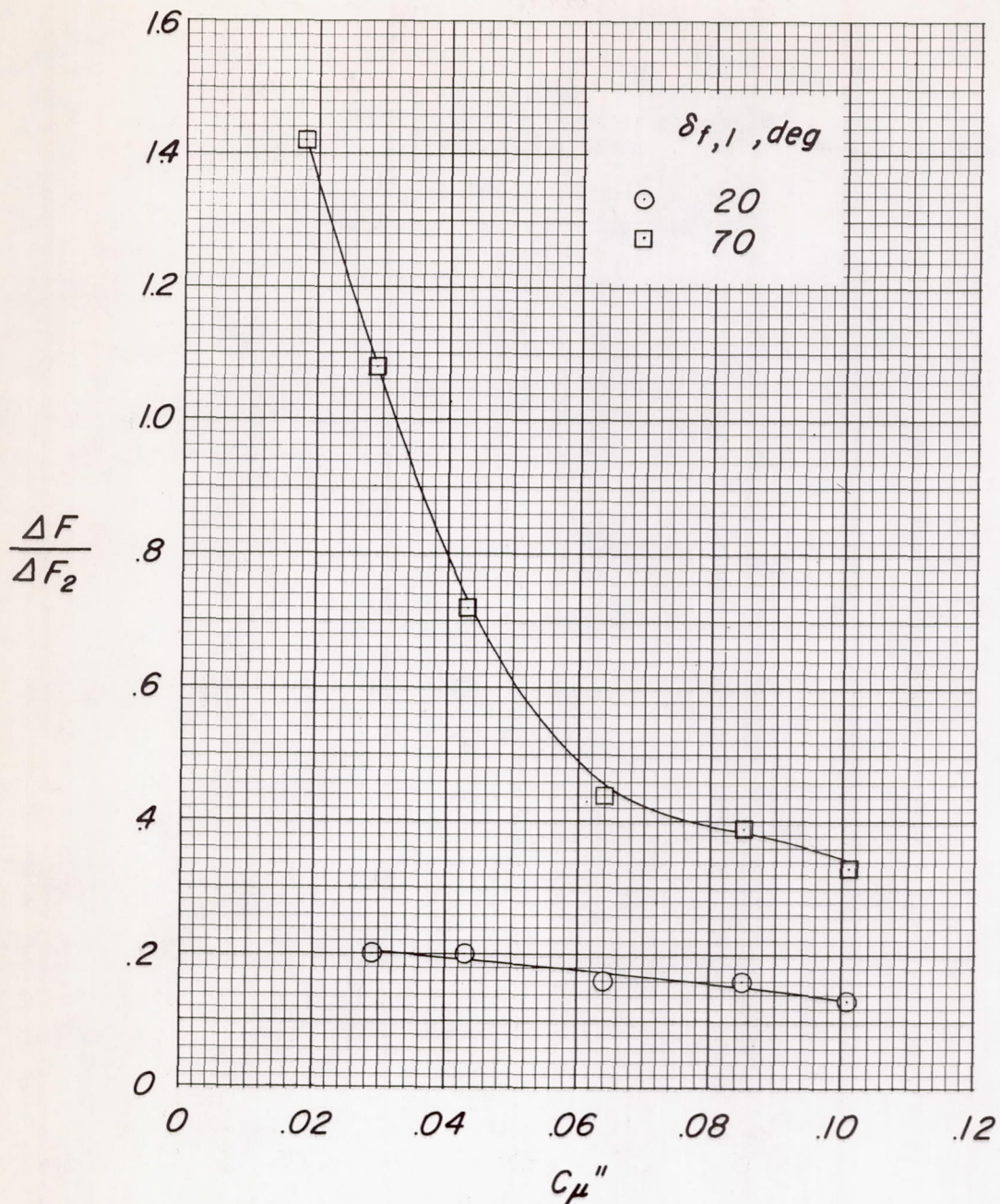
Figure 20.- Ratio of increment in resultant force obtained by blowing over the flap to the increment in resultant force obtained by utilizing the same power required by the blowing system in the propeller. $\eta'' = 0.75$; $\eta = 0.50$; $\delta_{f,2} = 0°$; $x/D = 0.41$; $z/D = 0$; $h/D = \infty$; nozzle gap, 0.016 inch.
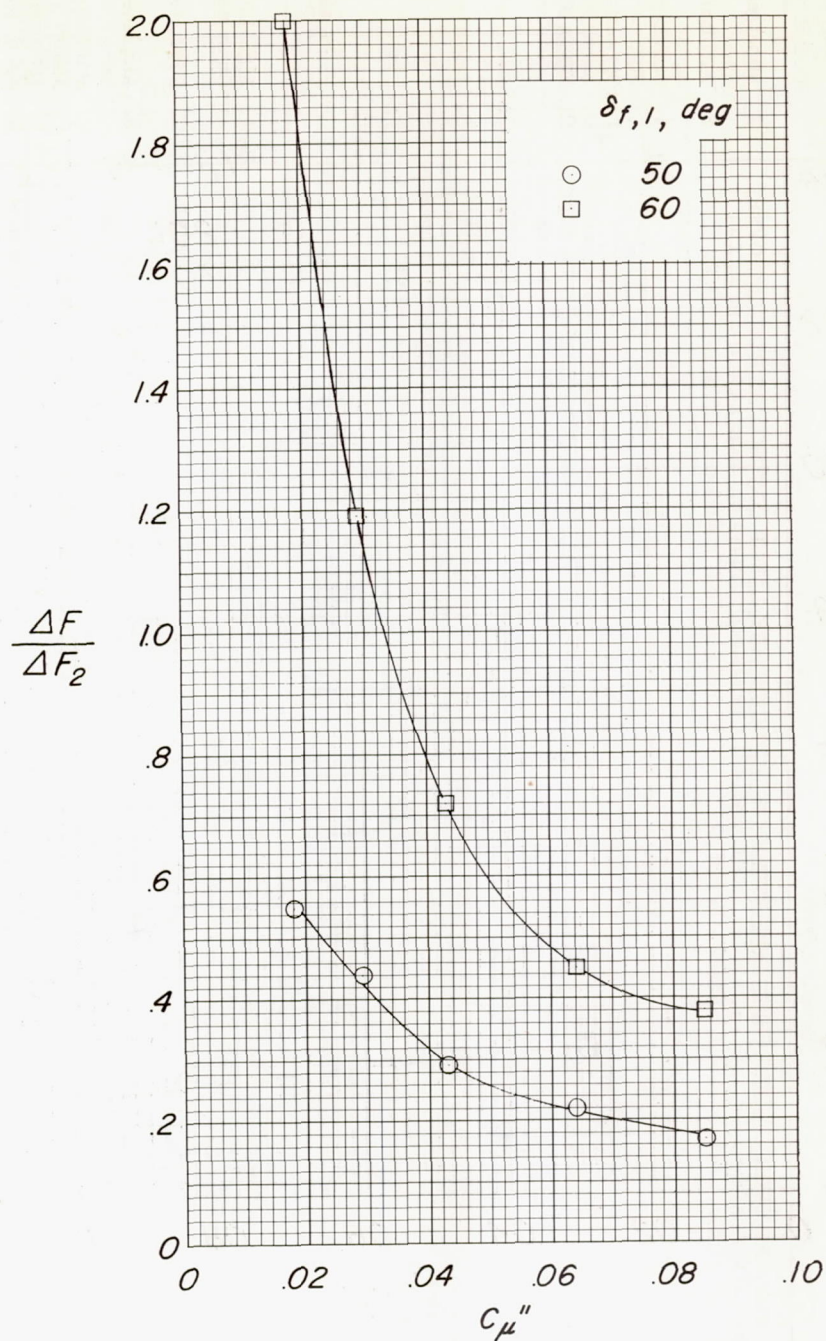
Figure 21.- Ratio of increment in resultant force obtained by blowing over flap to increment in resultant force obtained by utilizing same power required by blowing system in propeller. $\eta'' = 0.75$; $\eta = 0.50$; $\delta_{f,2} = 30°$; $x/D = 0.41$; $z/D = 0$; $h/D = \infty$; nozzle gap, 0.016 inch.